Provably Tightest Linear Approximation for Robustness Verification of Sigmoid-like Neural Networks

Zhaodi Zhang
zdzhang@stu.ecnu.edu.cn
East China Normal University
Shanghai, China

Yiting Wu
51205902026@stu.ecnu.edu.cn
East China Normal University
Shanghai, China

Si Liu
si.liu@inf.ethz.ch
ETH Zürich
Zürich, Switzerland

Jing Liu
jliu@sei.ecnu.edu.cn
Shanghai Key Laboratory of Trustworthy Computing,
East China Normal University
Shanghai, China

Min Zhang
zhangmin@sei.ecnu.edu.cn
East China Normal University,
Shanghai Institute of Intelligent Science and Technology
Shanghai, China

ABSTRACT

The robustness of deep neural networks is crucial to modern AI-enabled systems and should be formally verified. Sigmoid-like neural networks have been adopted in a wide range of applications. Due to their non-linearity, Sigmoid-like activation functions are usually *over-approximated* for efficient verification, which inevitably introduces imprecision. Considerable efforts have been devoted to finding the so-called *tighter* approximations to obtain more precise verification results. However, existing tightness definitions are heuristic and lack theoretical foundations. We conduct a thorough empirical analysis of existing *neuron-wise* characterizations of tightness and reveal that they are superior only on specific neural networks. We then introduce the notion of *network-wise tightness* as a unified tightness definition and show that computing network-wise tightness is a complex non-convex optimization problem. We bypass the complexity from different perspectives via two efficient, provably tightest approximations. The results demonstrate the promising performance achievement of our approaches over state of the art: (i) achieving up to 251.28% improvement to certified lower robustness bounds; and (ii) exhibiting notably more precise verification results on convolutional networks.

CCS CONCEPTS

• **Software and its engineering** → *Formal software verification*; • **Theory of computation** → *Abstraction.*

ACM Reference Format:
Zhaodi Zhang, Yiting Wu, Si Liu, Jing Liu, and Min Zhang. 2022. Provably Tightest Linear Approximation for Robustness Verification of Sigmoid-like Neural Networks . In *37th IEEE/ACM International Conference on Automated Software Engineering (ASE '22), October 10–14, 2022, Rochester, MI, USA.* ACM, New York, NY, USA, 17 pages. https://doi.org/10.1145/3551349.3556907

ASE '22, October 10–14, 2022, Rochester, MI, USA

ACM ISBN 978-1-4503-9475-8/22/10…$15.00
https://doi.org/10.1145/3551349.3556907

1 INTRODUCTION

The reliability concerns about deep neural networks (DNNs) are increasing more drastically than ever, especially as such networks are being embedded into software systems to make them intelligent. Considerable efforts from both AI and software engineering communities have been devoted to achieving *robust* DNNs by leveraging testing and verification techniques [4, 12, 32, 40, 42, 47, 48, 54]. Among these attempts, formal methods have been demonstrated effective in offering certified robustness guarantees, giving birth to an emerging research field called *Trustworthy AI* [50]. One distinguishing feature of formal methods is that they could provide rigorous proofs of correctness automatically when the properties are satisfied or disprove them by counterexamples (i.e., witnesses to the violations) [3, 9]. Robustness is an important correctness property in DNN verification: Minor modifications to the neural network's inputs must *not* alter its outputs [7]. Guaranteeing robustness is indispensable to prevent AI-enabled systems from environmental perturbations and adversarial attacks.

Formal robustness verification of DNNs has been well studied in recent years [14, 16, 20, 32, 33, 42, 45, 47–49]. Most efforts are focused on the *ReLU networks* that only use the simple piecewise ReLU activation function. Despite their wide adoptions in modern AI-enabled systems, another notable class of S-shaped (or Sigmoid-like) activation functions, such as Sigmoid, Tanh, and Arctan, have not attracted much attention yet. Due to their non-linearity, Sigmoid-like activation functions are far more complex to be verified. A *de facto* solution is to over-approximate such functions by linear bounds and to transform the verification problem into efficiently solvable linear programming. Many state-of-the-art DNN verification techniques, e.g., abstract interpretation [16, 40], symbolic interval propagation [45], model checking [33], differential verification [32], reachability and output range analysis [13, 44], are based on linear approximation.

Over-approximation inevitably introduces imprecision, rendering approximation-based verification incomplete: *Unknown* results may be returned when the neural network's robustness cannot be verified. Considerable efforts have been devoted to finding the so-called *tighter* approximations to achieve more precise verification results. For example, a larger certified lower robust bound [5, 28]

(the perturbation distance under which a neural network is proved robust against any allowable perturbation) is preferable in approximation. Several characterizations of tightness and approximation approaches have been proposed for Sigmoid-like activation functions [5, 18, 26, 28, 51, 55]. However, they are all heuristic and lack theoretical foundations for the individual outperformance.

We conduct a thorough empirical analysis of existing approaches and reveal that they are superior only on specific neural networks. In particular, we have found that the claimed tighter approximation actually produces smaller certified lower bounds according to the tightness defined and observed frequent occurrences of such cases.

Motivated by these observations, we introduce the notion of *network-wise tightness* as a *unified* tightness definition to characterize linear approximations of Sigmoid-like activation functions. This new definition ensures that a tighter approximation can always compute larger certified lower bounds (i.e., larger safe radius). However, we show that it unfortunately implies that computing the tightest approximation is essentially a network-wise non-convex optimization problem [28], which is hard to solve in practice [31].

We bypass the complex optimization problem from two different perspectives, depending on the neural network architecture. For the networks *with only one hidden layer*, we leverage a gradient-based searching algorithm for computing the tightest approximations. Regarding the networks *with multiple hidden layers*, based on our empirically study of the state-of-the-art tools, we have gained an insight that *a larger robust bound can be computed when the intervals keep to be tighter during the layer-by-layer propagation*. Based on this insight, we propose a *neuron-wise* tightest approximation and prove that it guarantees the *network-wise tightest approximation* when the networks are of non-negative weights. Such networks have been demonstrated suitable in a wide range of applications such as effective defense for adversarial attacks in malware and spam detection [8, 15, 19] and balancing accuracy and robustness in autoencoding [1, 29].

We have implemented a prototype of our approach called NeWise[1] and extensively compared it to three state-of-the-art tools, namely DeepCert [51], VeriNet [18], and RobustVerifier [26]. Our experimental results show that NeWise (i) achieves up to 251.28% improvement to certified lower robustness bounds in the provably tightest cases and (ii) exhibits up to 122.22% improvement to certified lower robustness bounds on convolutional networks.

To summarize, this paper makes three major contributions:

(1) We have introduced a novel unified definition of *network-wise tightness* to characterize the tightness of linear approximations for neural network robustness verification.
(2) We have identified two cases where we can efficiently achieve provably tightest approximations; the corresponding approaches have been proposed.
(3) We have implemented a verification tool and conducted comprehensive evaluation on its effectiveness and efficiency over three state-of-the-art verifiers.

The remainder of this paper proceeds as follows: Section 2 gives preliminaries on robustness verification of neural networks. Section 3 shows the tightness measurements of linear approximations and introduce our notion of network-wise tightness. Sections 4 and 5 present our provably tightest approximations from two different perspectives, respectively. Section 6 describes our evaluation results. We discuss related work in Section 7 and conclude in Section 8.

[1]Our code is available at https://github.com/FormalAIze/NeWise.git.

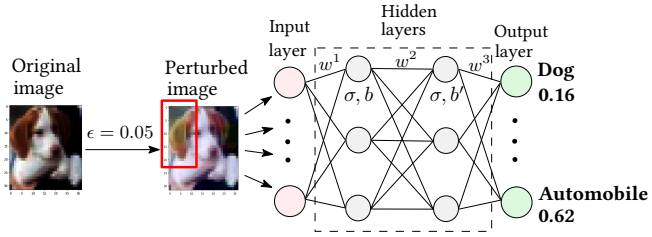

Figure 1: A perturbed image of a dog is misclassified to an automobile with 62% probability in 0.05 perturbation radius.

2 PRELIMINARIES

2.1 Robustness Verification of Neural Networks

2.1.1 Deep Neural Network. A deep neural network is a directed network, where the nodes are called neurons and arranged layer by layer. Each neuron is associated with an activation function $\sigma(x)$ and a bias b. Except for the first layer, the neurons on a layer are connected to those on the preceding layer, as shown in Figure 1. Every edge is associated with a weight, which is computed by training. The first and last layers are called input and output layers, respectively. The others between them are called hidden layers.

The *execution* of a neural network follows the style of layer-by-layer propagation. Each neuron on the input layer admits a number. The number is multiplied by the weights on the edges and then passed to the successor neurons on the next layer. All the incoming numbers are summed. The summation is fed to the activation function σ and the output of σ is added with the bias b. The result is then propagated to the next layer until reaching the output layer.

Formally, a k-layer neural network is a function $f : \mathbb{R}^n \to \mathbb{R}^m$ of the form $f^k \circ \sigma^{k-1} \circ \ldots \circ \sigma^1 \circ f^1$, with σ^t being a non-linear and differentiable activation function for t-th layer. The function f^t is either an affine transformation *or* a convolutional operation:

$$f(x) = Wx + b, \qquad \text{(Affine Transformation)}$$
$$f(x) = W * x + b, \qquad \text{(Convolutional Operation)}$$

where W, b, and $*$ refer to the weight matrix, the bias vector, and the convolutional product, respectively. In this work, we focus on the networks with the Sigmoid-like activation functions i.e., Sigmoid, Tanh, and Arctan, which are defined as follows, respectively.

$$\sigma(x) = \frac{1}{1+e^{-x}}, \qquad \sigma(x) = \frac{e^x - e^{-x}}{e^x + e^{-x}}, \qquad \sigma(x) = tan^{-1}(x)$$

The output of a neural network f is a vector of m floating numbers between 0 and 1, denoting the probabilities of classifying an input to the m labels. Let S be the set of m classification labels for the network f. We use $\mathcal{L}(f(x))$ to represent the output label for the input x with

$$\mathcal{L}(f(x)) = \arg\max_{s \in S} f(x)[s].$$

Intuitively, $\mathcal{L}(f(x))$ returns a label s in S such that $f(x)[s]$ is maximal among the numbers in the output vector.

2.1.2 Robustness and Robustness Verification. Neural networks are essentially "programs" composed by computers by fine-tuning the weights in the networks from training data. Unlike the handcrafted programs developed by programmers, neural networks lack formal requirements and are almost inexplicable, making it very challenging to formalize and verify their properties.

A neural network is called *robust* if reasonable perturbations to its inputs do not alter the classification result. A perturbation is typically measured by the distance between the perturbed input x' and the original one x by using ℓ_p-norm, denoted by $||x - x'||_p \triangleq \sqrt[p]{|x_1 - x'_1|^p + \ldots + |x_n - x'_n|^p}$, where p can be 1, 2 or ∞, and n is the length of the vectors x. In this work, we consider the most general case when $p = \infty$.

Example 1. We consider an example to explain how a perturbed image is misclassified. As shown in Figure 1, a normal image of a dog can be correctly classified by a neural network. We assume that the image can be perturbed within a 0.05 distance under ℓ_∞-norm. There exists a perturbed image such that when it is fed into the network, the outputs of the two neurons labeled by *dog* and *automobile* are 0.16 and 0.62, respectively. It indicates that the image is classified to a dog (resp. automobile) with the probability of 16% (reps. 62%). Therefore, it is classified to be an automobile, although it still represents a dog to human eyes, apparently.

The robustness of a neural network can be quantitively measured by a lower bound ϵ, which refers to a safe perturbation distance such that any perturbations below ϵ have the same classification result as the original input to the neural network.

Definition 1 (Local Robustness). *Given a neural network f, an input x_0, and a bound ϵ under ℓ_p-norm, f is called robust w.r.t. x_0 iff $\mathcal{L}(f(x)) = \mathcal{L}(f(x_0))$ holds for each x such that $||x - x_0||_p \leq \epsilon$. Such ϵ is called a certified lower bound.*

The twin problems of verifying f's robustness are: (i) to prove that, for each x satisfying $||x - x_0||_p \leq \epsilon$,

$$f_{s_0}(x) - f_s(x) > 0 \tag{1}$$

holds for each $s \in S - \{s_0\}$, where $s_0 = \mathcal{L}(f(x_0))$ and $f_s(x)$ returns the probability, i.e., $P(\mathcal{L}(f(x)) = s)$, of classifying x to the label s by f; and (ii) to compute a certified lower bound — a larger certified lower bound implies a more precise robustness verification result. As directly computing ϵ is difficult due to the non-linearity of the constraint (1), most of the state-of-the-art approaches [5, 51, 55] adopt the efficient binary search algorithm to first determine a candidate ϵ and then check whether (1) is true or false on ϵ.

2.2 Approximation-based Robustness Verification

A neural network f is highly non-linear due to the inclusion of activation functions. Proving Formula (1) is computationally expensive, e.g., NP-complete even for the simplest fully connected ReLU networks [20, 37]. Many approaches have been investigated to improve the verification efficiency while sacrificing completeness. Representative methods include interval analysis [46], abstract interpretation [16, 40], and output range estimation [13, 52], etc. The technique underlying these approaches is to over-approximate the non-linear activation functions using linear constraints, which can be more efficiently solved than the original ones.

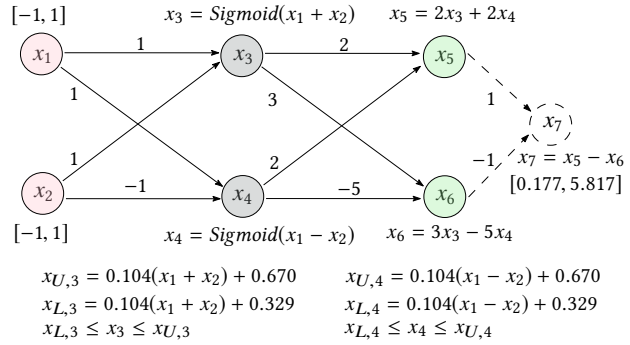

Figure 2: An example of approximation-based verification.

Instead of directly proving Formula (1), the approximation-based approaches over-approximate both $f_{s_0}(x)$ and $f_s(x)$ by two linear constraints and prove that the lower linear bound $f_{L,s_0}(x)$ of $f_{s_0}(x)$ is greater than the upper linear bound $f_{U,s}(x)$ of $f_s(x)$. Apparently, $f_{L,s_0}(x) - f_{U,s}(x) > 0$ is a sufficient condition of Formula (1), and it is significantly more efficient to prove or disprove. Therefore, it is widely adopted in neural network verification [5, 18, 26, 51], although it may produce false positives when it is disproved.

Definition 2 (Upper/Lower linear bounds). *Let $\sigma(x)$ be a non-linear function with $x \in [l, u]$, $\alpha_L, \alpha_U, \beta_L, \beta_U \in \mathbb{R}$, and*

$$h_U(x) = \alpha_U x + \beta_U, \qquad h_L(x) = \alpha_L x + \beta_L. \tag{2}$$

$h_U(x)$ and $h_L(x)$ are called upper and lower linear bounds of $\sigma(x)$ if the following condition holds:

$$\forall x \in [l, u], \quad h_L(x) \leq \sigma(x) \leq h_U(x). \tag{3}$$

Over-approximating the non-linear activation functions using linear lower and upper bounds is the key to the approximation of a neural network. For each activation function σ on a domain $[l, u]$, we define an upper linear bound h_U and a lower one h_L to ensure that for all x in $[l, u]$, $\sigma(x)$ is enclosed in $[h_L(x), h_U(x)]$.

Given an input range as in Definition 1, the output ranges of a network are computed by propagating the output interval of each neuron as in Definition 2 to the output layer.

Example 2. We consider an example of verifying a simple neural network based on approximation, as shown in Figure 2. The original verification problem is to prove that for any input (x_1, x_2) with $x_1 \in [-1, 1]$ and $x_2 \in [-1, 1]$, it is always classified to the label of neuron x_5. That is equivalent to proving that the output of the auxiliary neuron $x_7 = (x_5 - x_6)$ is always greater than 0. We define the linear upper/lower bounds $x_{U,3}, x_{L,3}$ and $x_{U,4}, x_{L,4}$ to over-approximate x_3 and x_4, respectively. It suffices to prove that $x_{L,5} - x_{U,6} > 0$ is always true. We can over-estimate the output interval of $x_{L,5} - x_{U,6}$ is $[0.177, 5.817]$ using $x_{U,3}, x_{L,3}$ and $x_{U,4}, x_{L,4}$ and consequently prove the robustness of the network for all the inputs in $[-1, 1] \times [-1, 1]$.

Note that it is not necessary to approximate an activation function using only one linear upper or lower bound. One may consider piece-wise linear bounds made up of a sequence of linear segments to approximate the function more tightly by being closer to it. However, the piece-wise way causes the number of constraints to blow

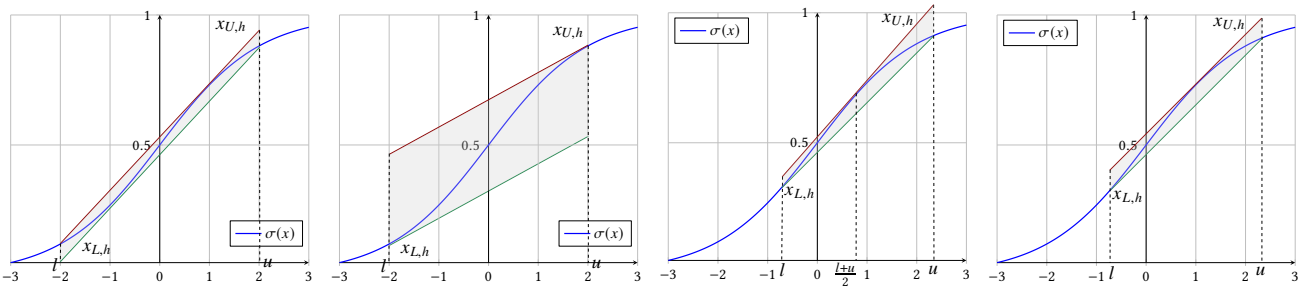

(a) Minimal area and parallel lines. **(b) Endpoints (our work).** **(c) Minimal area [18].** **(d) Parallel lines [51].**

Figure 3: Different approximations according to the domain of $\sigma(x)$ and their tightness definitions.

up exponentially when propagated layer by layer [40]. It would drastically reduce the verification scalability. Thus, over-approximating an activation function using one upper linear bound and one lower linear bound is the most efficient and widely-adopted choice for the approximation-based robustness verification approaches.

3 LINEAR APPROXIMATION APPROACHES

In this section, we analyze the tightness issue of existing approximation approaches and formally define a unified network-wise tightness to characterize the approximations. The network-wise tightness guarantees that output neurons can produce precise output ranges.

3.1 The Tightness Issue of Approximations

As approximation inevitably introduces overestimation, defining the *tightest* possible approximation is crucial to obtaining precise verification results. Several approximation approaches have been proposed under different strategies.

Henriksen et al. [18] proposed to measure the tightness of approximations using the enclosed area between the bound and the approximated function. An approximation is tighter if the corresponding area is smaller than another. By this definition, the approximations to x_3, x_4 should be the following linear bounds:

$$x'_{U,3} = 0.204(x_1 + x_2) + 0.527, \quad (4)$$

$$x'_{L,3} = 0.204(x_1 + x_2) + 0.472, \quad (5)$$

$$x'_{U,4} = 0.204(x_1 - x_2) + 0.527, \quad (6)$$

$$x'_{L,4} = 0.204(x_1 - x_2) + 0.472. \quad (7)$$

Figure 3a shows the bounds graphically. Apparently, they are closer to the activation function on the interval $[-2, 2]$. Surprisingly, using the *tighter* linear bounds the output range of x_7 is $[-0.079, 6.073]$, by which we cannot prove and disprove the robustness. Wu and Zhang adopted the same strategy for this case in their recent work [51]. In Example 2, we adopt a new strategy by taking the tangent lines at the two endpoints as its upper and lower bounds, as shown in Figure 3b. We obtain a smaller output range by these bounds, although they are far less tight than the one in Figure 3a.

In another case shown in Figure 3c, Henriksen et al. [18] proved that the tangent line at the middle point when $x = \frac{l+u}{2}$ is the tight upper bound because the enclosed area between it and the activation function is minimal. In Wu and Zhang's approach, they adopted the tangent line that is parallel to the lower bound as its upper bound, as shown in Figure 3d. Some other approaches such as [5, 26, 55] adopt similar approximation strategies, but they have been experimentally proved not as tight as the ones in [18, 51].

Table 1: Tightness evaluation of state of the art: DeepCert[51], VeriNet[28], and RobustVerifier[26]. CNN_{t-c} denotes a CNN with t layers and c filters of size 3×3. The models are pre-trained [2, 40, 51] by, e.g., DeepPoly [40].

Dataset	Model	#Neurons	Certified Lower Bound (Average)		
			DeepCert	VeriNet	Rob.Ver.
MNIST	3x50	160	0.0076	0.0077	0.0065
	3x100	310	0.0086	0.0087	0.0074
	3x200	610	0.0091	0.0092	0.0079
	5x100	510	0.0061	0.0062	0.0052
	6x500	3,010	0.0778	0.0776	0.0665
	CNN_{3-2}	2,514	0.0579	0.0580	0.0569
	CNN_{3-4}	5,018	0.0473	0.0472	0.0464
	CNN_{4-5}	8,680	0.0539	0.0543	0.0522
	CNN_{5-5}	10,680	0.0548	0.0550	0.0513
	CNN_{6-5}	12,300	0.0590	0.0588	0.0541
	CNN_{8-5}	14,570	0.0878	0.0882	0.0685
Fashion MNIST	3x50	160	0.0101	0.0102	0.0086
	5x100	510	0.0078	0.0079	0.0066
	CNN_{4-5}	8,680	0.0721	0.0720	0.0666
	CNN_{5-5}	10,680	0.0676	0.0677	0.0605
	CNN_{6-5}	12,300	0.0695	0.0691	0.0627
CIFAR10	3x50	160	0.0045	0.0046	0.0042
	5x100	510	0.0038	0.0037	0.0033
	CNN_{3-2}	3,378	0.0312	0.0313	0.0311
	CNN_{6-5}	17,110	0.0224	0.0223	0.0212

Lyu et al. [28] proposed a gradient-based searching approach for computing a tighter approximation if the approximation can produce tighter input intervals for the following neurons. However, the experimental results in the work [51] show that this approach neither guarantees it always produces larger certified lower robust bound than other approaches and its scalability is rather limited due to the complexity of the searching algorithm for each neuron.

Table 1 shows the comparison results, where, surprisingly, none of these approaches surpass the others for all the networks. We also observe that VeriNet won the competition on 13 out of 20 networks, while DeepCert on the remaining ones. This indicates that the performances of these so-called tight approaches vary case by case. In this paper we do not intend to judge which approach is better experimentally but focus on seeking theoretical foundations for the tightness of approximations. The comparison result showed that existing tightness definitions do not rigorously guarantee that a tighter approximation can always produce a larger robust bound. This motivates us to seek a unified definition to characterize the

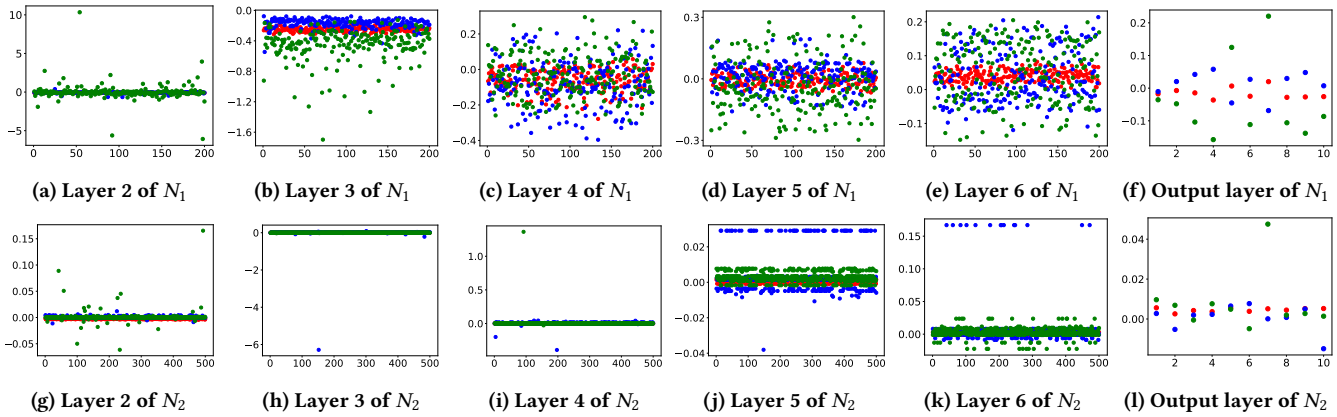

(a) Layer 2 of N_1 (b) Layer 3 of N_1 (c) Layer 4 of N_1 (d) Layer 5 of N_1 (e) Layer 6 of N_1 (f) Output layer of N_1

(g) Layer 2 of N_2 (h) Layer 3 of N_2 (i) Layer 4 of N_2 (j) Layer 5 of N_2 (k) Layer 6 of N_2 (l) Output layer of N_2

Figure 4: Visualization of intermediate intervals during layer-by-layer propagation under different approximations (Red dot: $\frac{(u-l)-(u'-l')}{u'-l'}$; blue dot: $\frac{l-l'}{l'}$; green dot: $\frac{u-u'}{u'}$; $[l,u]$: interval computed by VeriNet, $[l',u']$: interval computed by DeepCert).

tightness of approximations for robustness verification of neural networks.

3.2 Empirical Analysis

To validate our observation on the tightness issue and investigate its generality, we have performed empirical analysis of three state-of-the-art approximation approaches, i.e., DeepCert [51], VeriNet [18], and RobustVerifier [26], on 20 sigmoid neural networks collected from the public benchmarks. We evaluate the tightness of these approaches by computing the lower robust bound for each network using the tools, respectively. We randomly selected 100 images for each network, computed their lower robust bounds, and took the average value. Computing averaged lower bounds is a widely-adopted approach to reduce the affect of floating-point errors [28, 47, 51]. Thus, even a small difference in the averaged value reflects a big difference in individual input. In general, the larger bound indicates the corresponding tool has a better performance.

We empirically analyzed the layer-by-layer propagation in the verification process of the best two tools VeriNet and DeepCert and identified the missing factor that influences verification results. We tracked the computation of the intermediate intervals of the neurons on hidden layers during their layer-by-layer propagation and compared their tightness under different approximation strategies.

Figure 4 shows the layer-by-layer comparison of the intermediate intervals on the hidden neurons and output neurons. These intervals are computed during verification using the approximation approaches in [18, 51], respectively. The figures from Figure 4a to 4f show one 5-hidden-layer network named N_1 on which VeriNet computes a larger bound than DeepCert, while those from Figure 4g to 4l show another 5-hidden-layer network named N_2 on which DeepCert computes a larger bound than VeriNet. For each neuron, we use $[l,u]$ and $[l',u']$ to represent the intervals computed by VeriNet and DeepCert, respectively. We introduce three dots in red, blue and green to represent $\frac{(u-l)-(u'-l')}{u'-l'}$, $\frac{l-l'}{l'}$ and $\frac{u-u'}{u'}$, respectively. The x-axis represents the neurons on the corresponding layer, and the y-axis represents the differences of the interval length, lower bounds, and upper bounds of the intervals.

Horizontally on N_1, most of the red dots are below 0 from layer 2 to the output layer, except layer 6. That indicates the intervals computed by VeriNet usually have smaller (tighter) sizes than those by DeepCert. The blue dots gradually move up above 0, indicating that the lower bounds of the intervals computed by VeriNet become greater than the those by DeepCert. Similarly, the green dots gradually move down below 0, indicating that the upper bounds computed by VeriNet become smaller. The trends of the three values reflect that the intermediate intervals computed by VeriNet are statistically tighter than those by DeepCert on network N_1.

The trend of intermediate intervals on network N_2 is an opposite of the one on N_1. The red dots move up above 0 layer by layer, indicating that the interval sizes computed by VeriNet become larger than those by DeepCert. The blue dots gradually move down below 0 and the green ones move up above 0.

The analysis result from Figure 4 reveals that the intermediate intervals are statistically tighter than other tools when a tool produces larger certified lower bounds.

3.3 The Network-Wise Tightest Approximation

Existing characterizations of tightness are individually heuristic under a presumption that a tighter approximation gives rise to a more precise verification result. Unfortunately, the above examples show that this presumption does not always hold. It means that defining the tightness on each individual neuron is neither sufficient nor necessary for achieving tight approximations. That is because the tightness on neurons cannot guarantee the output intervals of neural networks are always precise. However, the output intervals are the basis for judging whether a network is robust or not.

To characterize the tightness of approximations to the activation functions in a neural network, we introduce the notion of *network-wise tightness*. We ensure that, by a network-wise tighter approximation of the activation functions, the approximated neural network must produce more precise output intervals and consequently more precise verification results.

Definition 3 (Network-wise tightness). *Given a neural network $f : \mathbb{R}^n \to \mathbb{R}^m$ and $x \in \mathbb{B}_p(x_0, \epsilon)$, let (f_L, f_U) be a linear*

approximation of f with f_U and f_L the upper and lower bounds, respectively. (f_L, f_U) is network-wise tightest if, for any different linear approximation $(\hat{f}_L, \hat{f}_U)$,

$$\forall s \in S, \quad \min_{x\in\mathbb{B}_p(x_0,\epsilon)} f_{L,s}(x) \geq \min_{x\in\mathbb{B}_p(x_0,\epsilon)} \hat{f}_{L,s}(x),$$
$$\max_{x\in\mathbb{B}_p(x_0,\epsilon)} f_{U,s}(x) \leq \max_{x\in\mathbb{B}_p(x_0,\epsilon)} \hat{f}_{U,s}(x),$$

where $f_{L,s}(x), f_{U,s}(x)$ denote s-th item of $f_L(x), f_U(x)$, respectively.

Intuitively, (f_L, f_U) is tighter than $(\hat{f}_L, \hat{f}_U)$ in that for all output neurons s, f_L (*resp.* f_U) always computes a lower (*resp.* an upper) bound that is greater (*resp.* less) than the one $\hat{f}_L$ (*resp.* $\hat{f}_U$) does. Note that Definition 3 is universal in that it is applicable to (i) all activation functions and (ii) all ℓ_p norms.

Example 3. By Definition 3, the approximations $x_{U,3}, x_{L,3}, x_{U,4}, x_{L,4}$ to the activation functions on x_3 and x_4 in Example 2 are tighter than $x'_{U,3}, x'_{L,3}, x'_{U,4}, x'_{L,4}$. This is consistent to the verification results. Using the former approximations, we can compute tighter output ranges for both x_5 and x_6 than those by the latter. However, the former approximation can be proved to be less tight than the latter if we take the tightness definition with respect to the minimal area defined in [18].

Next, we give an important property of the network-wise tightness. That is, a network-wise tighter approximation always leads to more precise verification results.

Theorem 1. *The approximation (f_L, f_U) of a neural network always produces more precise robustness verification result than $(\hat{f}_L, \hat{f}_U)$ if (f_L, f_U) is tighter than $(\hat{f}_L, \hat{f}_U)$ by Definition 3.*

Proof sketch. Let $s_0 = \mathcal{L}(f(x_0))$ with fixed ϵ. We check for all s other than s_0 whether the following condition:

$$\min_{x\in\mathbb{B}_p(x_0,\epsilon)} f_{L,s_0}(x) > \max_{x\in\mathbb{B}_p(x_0,\epsilon)} f_{U,s}(x) \tag{8}$$

holds. By Definition 3, if $(\hat{f}_L, \hat{f}_U)$ satisfies (8), then we have:

$$\min_{x\in\mathbb{B}_p(x_0,\epsilon)} f_{L,s_0}(x) \geq \min_{x\in\mathbb{B}_p(x_0,\epsilon)} \hat{f}_{L,s_0}(x) >$$
$$\max_{x\in\mathbb{B}_p(x_0,\epsilon)} \hat{f}_{U,s}(x) \geq \max_{x\in\mathbb{B}_p(x_0,\epsilon)} f_{U,s}(x),$$

for all s other than s_0. Thus, (f_L, f_U) certainly satisfies (8) as well. Namely, the result verified by $(\hat{f}_L, \hat{f}_U)$ can also be deduced by (f_L, f_U). On the contrary, the result verified by (f_L, f_U) may not be verified by $(\hat{f}_L, \hat{f}_U)$. Consequently, (f_L, f_U) always produce more precise verification result than $(\hat{f}_L, \hat{f}_U)$. □

Next, we show that computing the network-wise tightest approximation is essentially an optimization problem. Given a k-layer neural network $f : \mathbb{R}^n \to \mathbb{R}^m$, we use ϕ^t to denote the compound function of f's layers before t-th activation function is applied, *i.e.,*

$$\phi^t = f^t \circ \sigma^{t-1} \circ f^{t-1} \circ \ldots \circ \sigma^1 \circ f^1.$$

For layer t with n^t neurons, let $\phi^t_r(x)$ indicate r-th item of its output (with $r \in \mathbb{Z}$ and $1 \leq r \leq n^t$). For each activation function $\sigma(x)$ with $x \in [l, u]$, we denote the upper (resp. lower) bound of $\sigma(x)$ by $h_U(x) = \alpha_U x + \beta_U$ (resp. $h_L(x) = \alpha_L x + \beta_L$), with variables $\alpha_L, \alpha_U, \beta_L, \beta_U \in \mathbb{R}$. The problem of computing the network-wise tightest approximation can then be formalized as the following optimization problems:

$$\max(\min_{x\in\mathbb{B}_\infty(x_0,\epsilon)} (A^k_{L,s}x + B^k_{L,s})), \text{and} \tag{9}$$
$$\min(\max_{x\in\mathbb{B}_\infty(x_0,\epsilon)} (A^k_{U,s}x + B^k_{U,s})) \tag{10}$$
$$s.t. \quad \forall r \in \mathbb{Z}, 1 \leq r \leq n^t, \forall t \in \mathbb{Z}, 1 \leq t < k,$$
$$\begin{cases} \alpha^t_{L,r} z^t_r + \beta^t_{L,r} \leq \sigma(z^t_r) \leq \alpha^t_{U,r} z^t_r + \beta^t_{U,r}; \\ \min\limits_{x\in\mathbb{B}_\infty(x_0,\epsilon)} A^t_{L,r}x + B^t_{L,r} \leq z^t_r \leq \max\limits_{x\in\mathbb{B}_\infty(x_0,\epsilon)} A^t_{U,r}x + B^t_{U,r}. \end{cases}$$

Here, $A^t_{L,r}x + B^t_{L,r}$ and $A^t_{U,r}x + B^t_{U,r}$ are the lower and upper linear bounds of $\phi^t_r(x)$, respectively. $A^t_{L,r}, A^t_{U,r}, B^t_{L,r}$ and $B^t_{U,r}$ are constant tensors defined on W^t, b^t, where W^t, b^t are the weights and biases of the t-th layer. ϕ^t_r is the compound function of f's first t layers. $\phi^t_r(x)$ can be approximated by a lower linear bound $A^t_{L,r}x + B^t_{L,r}$ and an upper linear bound $A^t_{U,r}x + B^t_{U,r}$ with:

$$A^t_{L,r} = \begin{cases} W^t_r, & t = 1 \\ W^t_{\geq 0,r}\alpha^{t-1}_L \odot A^{t-1}_L + W^t_{<0,r}\alpha^{t-1}_U \odot A^{t-1}_L, & t \geq 2 \end{cases}$$
$$B^t_{L,r} = \begin{cases} b^t_r, & t = 1 \\ W^t_{\geq 0,r}(\alpha^{t-1}_L \odot B^{t-1}_L + \beta^{t-1}_L) + \\ W^t_{<0,r}(\alpha^{t-1}_U \odot B^{t-1}_L + \beta^{t-1}_L) + b^t_r, & t \geq 2 \end{cases}$$
$$A^t_{U,r} = \begin{cases} W^t_r, & t = 1 \\ W^t_{\geq 0,r}\alpha^{t-1}_U \odot A^{t-1}_U + W^t_{<0,r}\alpha^{t-1}_L \odot A^{t-1}_U, & t \geq 2 \end{cases}$$
$$B^t_{U,r} = \begin{cases} b^t_r, & t = 1 \\ W^t_{\geq 0,r}(\alpha^{t-1}_U \odot B^{t-1}_U + \beta^{t-1}_U) + \\ W^t_{<0,r}(\alpha^{t-1}_L \odot B^{t-1}_U + \beta^{t-1}_U) + b^t_r, & t \geq 2 \end{cases}$$

where $\odot$ denotes Hadamard production.

The solutions to all $\alpha_L, \alpha_U, \beta_L, \beta_U$ are the linear bounds to all the activation functions in the network, and their composition is the network-wise tightest approximation. Note that the solutions may not guarantee that the approximation to an individual activation function is the tightest with respect to existing tightness definitions.

4 APPROACH FOR 1-HIDDEN-LAYER NETWORKS

Given a neural network, we can compute the network-wise tightest approximation by instantiating and solving the optimization problems (9) and (10). For a one-hidden-layer network, the optimization problems can be simplified as follows:

$$\max(\min_{x\in\mathbb{B}_\infty(x_0,\epsilon)} (A_{L,s}x + B_{L,s})), \tag{11}$$
$$\min(\max_{x\in\mathbb{B}_\infty(x_0,\epsilon)} (A_{U,s}x + B_{U,s})), \tag{12}$$
$$s.t. \quad \forall r \in \mathbb{Z}, 1 \leq r \leq n,$$
$$\begin{cases} \alpha_{L,r} z_r + \beta_{L,r} \leq \sigma(z_r) \leq \alpha_{U,r} z_r + \beta_{U,r}; \\ \min\limits_{x\in\mathbb{B}_\infty(x_0,\epsilon)} W^1 x + b^1 \leq z_r \leq \max\limits_{x\in\mathbb{B}_\infty(x_0,\epsilon)} W^1 x + b^1. \end{cases}$$

where $A_{L,s} = W^2_{\geq 0,s}(\alpha_L \odot W^1) + W^2_{<0,s}(\alpha_U \odot W^1)$, $B_{L,s} = W^2_{\geq 0,s}(\alpha_L \odot b^1 + \beta_L) + W^2_{<0,s}(\alpha_U \odot b^1 + \beta_U) + b^2_s$, n denotes the amount of neurons in the hidden layer. The above optimization problems are the instances of the problems (9) and (10).

Algorithm 1: A gradient descent-based searching algorithm for the tightest approximations of 1-hidden-layer networks.

Input : N: a network; x_0: an input to N; ϵ: a ℓ_∞-norm radius
Output: $\alpha_{L,r}, \beta_{L,r}, \alpha_{U,r}, \beta_{U,r}$ for each hidden neuron r

1 **for** *each neuron* r **do**
2 Evaluate input range $[l_r, u_r]$ for r;
3 Let ω denote the line connecting $(l_r, \sigma(l_r))$ and $(u_r, \sigma(u_r))$;
4 $R_L \leftarrow \emptyset, R_U \leftarrow \emptyset$; *// Empty the sets of optimizable neurons.*
5 **if** ω *can be an upper bound of* σ **then**
6 Let $\alpha_{U,r}, \beta_{U,r}$ be the slope and intercept of ω;
7 Add $(r, [l_r, u_r])$ to R_L; *// r's lower bound is optimizable.*
8 **else if** ω *can be a lower bound of* σ **then**
9 Let $\alpha_{L,r}, \beta_{L,r}$ be the slope and intercept of ω;
10 Add $(r, [l_r, u_r])$ to R_U; *// r's upper bound is optimizable.*
11 **else**
12 Let $z_{U,r}, z_{L,r}$ be the cut-off points of the tangent lines of σ crossing $(l_r, \sigma(l_r))$ and $(u_r, \sigma(u_r))$;
13 Add $(r, [z_{U,r}, u_r])$ to R_U, and $(r, [l_r, z_{L,r}])$ to R_L;
14 Randomize the cut-off points for optimizable bounds of r;
15 Let $\alpha_{L,r}, \beta_{L,r}, \alpha_{U,r}, \beta_{U,r}$ be the slope and intercept of tangent line of σ at chosen cut-off points;
16 **for** $1, \ldots, k$ **do** *// k is the preset optimization round*
17 Compute $A_{L,s}, B_{L,s}$ of the lower bound of output neuron s;
18 Let $G := \min_{x \in \mathbb{B}_\infty(x_0, \epsilon)} (A_{L,s}x + B_{L,s})$;
19 Update the cut-off points for r's bound through $-\nabla(G)$;
20 Update $\alpha_{L,r}, \beta_{L,r}, \alpha_{U,r}, \beta_{U,r}$ at chosen cut-off points;

The optimization problem is a convex variant and thus efficiently solvable by leveraging the gradient descent-based searching algorithm [28]. Algorithm 1 shows the pseudo code of the algorithm for calculating the optimal solution for the optimization problem with objective function (11). A solution represents a network-wise tightest lower bound to the 1-hidden-layer networks. For each activation function on a hidden neuron, it first determines whether the line ω crossing the two endpoints can be an upper (Lines 5-7) or lower bound (Lines 8-10). If those are the cases, the tangent line of the activation function is chosen to be lower bound (*resp.* upper bound), and its cut-off point can be an optimization variable. Otherwise (Lines 11-13), the lower and upper bounds can both be optimized. The optimizing ranges for those cases are calculated.

Let $G := \min_{x \in \mathbb{B}_\infty(x_0, \epsilon)} (A_{L,s}x + B_{L,s})$ and $ANS = \max_{\alpha_L, \alpha_U, \beta_L, \beta_U} (G)$. We use gradient descent steps (Lines 16-20) to optimize the target ANS. We conduct gradient descent and modify the value of $\alpha_L, \alpha_U, \beta_L, \beta_U$ if the ANS achieves a larger result under the new bounds.

The optimization problem with objective function (12) can be solved by the same algorithm, with ANS replaced by (12).

Example 4. Let us revisit Example 2. With Algorithm 1, we compute the network-wise tightest approximations for the network in Figure 2. Figure 5 shows the upper (*resp.* lower) bounds, denoted by $x''_{U,3}, x''_{U,4}$ (*resp.* $x''_{L,3}, x''_{L,4}$). By Definition 3, $x''_{U,3}, x''_{U,4}$ are tighter than the other two approximations. The resulting output range of neuron x_7 is $[0.307, 5.693]$, which is more precise than both $[-0.079, 6.073]$ and $[0.177, 5.817]$ in Figure 3a and 3b, respectively.

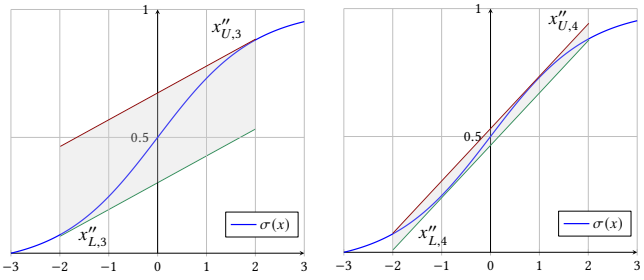

Figure 5: The network-wise tightest approximation to the activation functions on x_3 (left) and x_4 (right) in Example 2.

Note that the network-wise tightest approximations in the above example are a hybrid of both kinds of approximations in Figure 3a and 3b, which cannot be the tightest under a single tightness criterion in [18, 51]. This echoes our advocation that solely pursuing neuron-wise tightness under existing tightness definitions may not guarantee that they are the network-wise tightest, and consequently cannot achieve precise robust verification results.

5 APPROACH FOR MULTI-HIDDEN-LAYER NETWORKS

For the networks with two or more hidden layers, solving the optimization problems (9) and (10) becomes impractical due to its non-convexity. In [28], Lyu *et al.* proved that it is even non-convex to separately compute the tightest approximation for each neuron. The intractability lies in the accumulated constraints throughout the network: for any hidden layer, the input intervals of the activation functions are constrained by the approximations to the activation functions for the previous hidden layer. Neither can the optimization problems be solved on a layer basis because the objective function are network-wise. To our knowledge, no efficient algorithms or tools exist for such optimization problems. In this section, we propose computable neuron-wise tightest approximations and identify the condition when all the weights in a neural network are non-negative, the neuron-wise tightest approximations lead to being network-wise tightest.

5.1 The Neuron-Wise Tightest Approximation

Our empirical analysis in Section 3.1 reveals an insight that preserving tighter intermediate intervals during layer-by-layer propagation usually produces larger certified lower robust bounds. In the same spirit, we heuristically define the tightness of an approximation to an individual activation function in terms of the overestimation caused by the approximation. Smaller overestimation implies a tighter approximation. Particularly, an approximation is the *neuron-wise tightest* if it results in no overestimation of the output range of the activation function.

Definition 4 (Neuron-wise Tightness). *Let $\sigma(x)$ be an activation function with $x \in [l, u]$, and $h_U(x), h_L(x)$ be its upper and lower bounds, with α_U, α_L their slopes. $h_U(x)$ (resp. $h_L(x)$) is the neuron-wise tightest if $h_U(u) = \sigma(u)$ (resp. $h_L(l) = \sigma(l)$) and $\int_l^u h_U(x) - \sigma(x)dx$ (resp. $\int_l^u \sigma(x) - h_L(x)dx$) is minimal.*

By Definition 4, we identify three cases of defining the neuron-wise tightest approximation for each individual activation function.

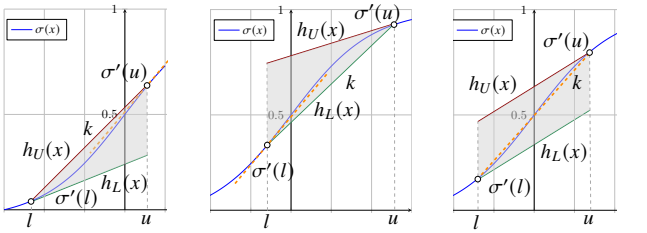

(a) $\sigma'(l) < k < \sigma'(u)$ **(b)** $\sigma'(l) > k > \sigma'(u)$ **(c)** $k > \sigma'(l) \wedge k > \sigma'(u)$

Figure 6: The neuron-wise tightest linear approximation.

The three cases are defined according to the relation between the slopes of activation function at two endpoints and the slope of the line crossing the two endpoints, as classified in [18, 51]. Given an input interval $[l, u]$ for $\sigma(x)$, the slopes of $\sigma(x)$ at $(l, \sigma(l))$ and $(u, \sigma(u))$ are represented by $\sigma'(l)$ and $\sigma'(u)$, respectively; the slope of the line crossing $(l, \sigma(l))$ and $(u, \sigma(u))$ is $k = \frac{\sigma(u)-\sigma(l)}{u-l}$. Figure 6 depicts the neuron-wise tightest approximations in the following three different cases:

Case 1. When $\sigma'(l) < k < \sigma'(u)$ (Figure 6a), the line that connects the two endpoints is chosen as the upper bound, while the tangent line of $\sigma(x)$ at $(l, \sigma(l))$ as the lower bound. We then have $h_U(x) = k(x - l) + \sigma(l)$ and $h_L(x) = \sigma'(l)(x - l) + \sigma(l)$.

Case 2. When $\sigma'(u) < k < \sigma'(l)$ (Figure 6b), the tangent line of $\sigma(x)$ at $(u, \sigma(u))$ and the line crossing two endpoints are considered as the upper and lower bounds, respectively. We then have $h_U(x) = \sigma'(u)(x - u) + \sigma(u)$ and $h_L(x) = k(x - u) + \sigma(u)$.

Case 3. When $\sigma'(l) < k$ and $\sigma'(u) < k$ (Figure 6c), the tangent line of $\sigma(x)$ at $(u, \sigma(u))$ is taken as the upper bound, while the tangent line of $\sigma(x)$ at $(l, \sigma(l))$ as the lower bound. We then have $h_U(x) = \sigma'(u)(x - u) + \sigma(u)$ and $h_L(x) = \sigma'(l)(x - l) + \sigma(l)$.

Note that, Definition 4 also considers the tightness characterizations in [18, 28]. It is easy to prove that any other linear bound crossing the endpoints is less tight than the one defined in the above three cases according to the tightness definitions in [18, 28].

5.2 Neuron-Wise vs. Network-Wise

In this section, we study the relation between neuron-wise tightness and network-wise tightness. Although the neuron-wise tightest approximation does not overestimate the output range of a single neuron, it cannot guarantee that the composition for all the neurons is the network-wise tightest because the monotonicity of a neuron cannot be preserved by the next layer. The monotonicity may be altered by the weights between layers because the input function of each neuron in any hidden layer is compounded by the output functions in the previous layer multiplied by the weights. Hence, a sufficient condition of passing neuron-wise tightness to the network is to avoid breaking monotonicity during the propagation.

Definition 5 (Network-wise monotonous). *Given a k-layer neural network $f : \mathbb{R}^n \to \mathbb{R}^m$ and its input $x = [x_1, ..., x_n]$, f is called network-wise monotonous if the following three conditions hold:*

(1) $\forall t_1, t_2 \in \mathbb{Z}, 1 \leq t_1 \leq k \wedge 1 \leq t_2 \leq k$,
(2) $\forall r_1, r_2 \in \mathbb{Z}, 1 \leq r_1 \leq n^{t_1} \wedge 1 \leq r_2 \leq n^{t_2}$,
(3) $\forall i \in \mathbb{Z}, 1 \leq i \leq n, \phi^{t_1}_{r_1}(x_i), \phi^{t_2}_{r_2}(x_i)$ *are both either monotonically increasing or decreasing.*

Intuitively, a monotonous network requires all the neurons to share the same monotonicity w.r.t. the input so that they can achieve the maximum or minimum on the same input.

Lemma 1. *A neural network is network-wise monotonous if the network satisfies the following two conditions:*

(1) *For the first layer, for any selected $i \in \mathbb{Z}, 1 \leq i \leq n$, items in the i-th column of W^1 are all positive or all negative;*
(2) *Every item in weights from the second layer to the last layer is non-negative.*

Next, we formulate the most important property of our neuron-wise approximation approach as the following theorem, stating that the composition of all neuron-wise tightest approximations is the network-wise tightest if the network is monotonous.

Theorem 2. *The composition of the neuron-wise tightest approximations is the network-wise tightest if the network satisfies the following two conditions:*

(1) *For the first layer, the items in each column of the weight matrix are all positive or negative;*
(2) *Every item in weights between remained layers is non-negative.*

Theorem 2 holds as both conditions guarantee the monotonicity of the network. If a neural network is monotonous, then the composition of the neuron-wise tightest approximations is a network-wise tightest approximation with respect to the robustness verification. In particular, starting from the second layer, the neuron-wise tightness is preserved with only non-negative weights during the layer-wise propagation (the second condition). See Appendix B for the complete proof.

Example 5. Assume that we replace the three negative weights of the neural network in Figure 2 with 1, 5, and 1, respectively. The tightest approximations to x_3 and x_4, returned by Algorithm 1, are exactly the same as those returned by the neuron-wise tightest approximations in Section 5.1 (i.e., $[1.430, 10.570]$).

6 EXPERIMENTS

We evaluate our approximation method concerning both precision and efficiency in the robustness verification of Sigmoid-like neural networks. Our goal is threefold:

(1) To validate our mathematical proof of Theorem 2 via extensive experimental results (i.e., always returning the largest certified lower bounds for non-negative networks);
(2) To demonstrate that Algorithm 1 can always compute tighter lower bounds for 1-hidden-layer networks;
(3) To explore our approach's effectiveness under general neural networks with *mixed* weights.

6.1 Benchmarks and Experimental Setup

Competitors. We consider three representative approximations in the literature: DeepCert [51], VeriNet [18], and RobustVerifier [26]. For a fair comparison, we implemented in Python all the competing approaches including our new algorithm called NeWise.

Datasets and Networks. We have conducted three sets of experiments on fully connected (FNNs) and convolutional (CNNs) networks: We focus on CNNs due to their effectiveness in a wide

Table 2: Performance comparison on non-negative Sigmoid networks between NeWise (NW) and existing tools, DeepCert (DC), VeriNet (VN), and RobustVerifier (RV). $t \times n$ refers to an FNN with t layers and n neurons per layer. CNN_{t-c} denotes a CNN with t layers and c filters of size 3×3.

Dataset	Model	#Neur.	Certified Lower Bound														Time (s)
			Average							Standard Deviation							
			NW	DC	Impr. (%)	VN	Impr. (%)	RV	Impr. (%)	NW	DC	Impr. (%)	VN	Impr. (%)	RV	Impr. (%)	
MNIST	5x100	510	0.0091	0.0071	28.15 ↑	0.0071	27.25 ↑	0.0064	40.90 ↑	0.0057	0.0042	37.11 ↑	0.0042	35.48 ↑	0.0034	69.35 ↑	4.30 ±0.02
	3x700	2,110	0.0037	0.0030	24.92 ↑	0.0030	22.85 ↑	0.0029	27.05 ↑	0.0018	0.0013	41.86 ↑	0.0014	34.56 ↑	0.0013	41.86 ↑	117.94 ±0.31
	CNN_{6-5}	12,300	0.0968	0.0788	22.82 ↑	0.0778	24.37 ↑	0.0699	38.50 ↑	0.0372	0.0280	32.92 ↑	0.0276	35.09 ↑	0.0212	75.86 ↑	5.70 ±0.42
	3x50	160	0.0105	0.0088	19.23 ↑	0.0088	19.50 ↑	0.0080	31.42 ↑	0.0051	0.0038	32.72 ↑	0.0038	32.72 ↑	0.0029	71.86 ↑	0.14 ±0.00
	3x100	310	0.0139	0.0120	15.46 ↑	0.0120	15.56 ↑	0.0111	25.47 ↑	0.0071	0.0057	24.82 ↑	0.0057	23.30 ↑	0.0046	53.46 ↑	2.22 ±0.02
	CNN_{5-5}	10,680	0.0801	0.0708	13.14 ↑	0.0704	13.75 ↑	0.0683	17.30 ↑	0.0238	0.0200	18.87 ↑	0.0198	20.50 ↑	0.0180	32.20 ↑	2.88 ±0.32
	CNN_{3-2}	2,514	0.0521	0.0483	7.82 ↑	0.0483	7.94 ↑	0.0478	8.88 ↑	0.0180	0.0161	12.13 ↑	0.0160	12.41 ↑	0.0156	15.44 ↑	0.17 ±0.04
	CNN_{4-5}	8,680	0.0505	0.0473	6.68 ↑	0.0471	7.26 ↑	0.0464	8.81 ↑	0.0207	0.0186	11.26 ↑	0.0183	12.84 ↑	0.0175	17.87 ↑	1.17 ±0.20
	CNN_{3-4}	5,018	0.0448	0.0422	6.09 ↑	0.0421	6.24 ↑	0.0418	6.98 ↑	0.0156	0.0142	9.71 ↑	0.0141	10.18 ↑	0.0138	12.56 ↑	0.30 ±0.08
Fashion MNIST	4x100	410	0.0312	0.0188	65.48 ↑	0.0194	60.62 ↑	0.0159	96.22 ↑	0.0403	0.0210	92.28 ↑	0.0220	83.20 ↑	0.0176	129.47 ↑	3.31 ±0.04
	3x100	310	0.0326	0.0263	24.02 ↑	0.0270	21.03 ↑	0.0238	36.81 ↑	0.0335	0.0262	27.67 ↑	0.0282	18.92 ↑	0.0234	43.22 ↑	2.22 ±0.01
	CNN_{5-5}	10,680	0.1303	0.1155	12.81 ↑	0.1151	13.22 ↑	0.1088	19.72 ↑	0.0830	0.0714	16.23 ↑	0.0721	15.10 ↑	0.0636	30.51 ↑	2.89 ±0.33
	CNN_{3-2}	2,514	0.0790	0.0713	10.79 ↑	0.0713	10.74 ↑	0.0695	13.68 ↑	0.0497	0.0416	19.55 ↑	0.0418	19.06 ↑	0.0386	28.98 ↑	0.17 ±0.04
	CNN_{4-5}	8,680	0.0959	0.0868	10.40 ↑	0.0864	10.90 ↑	0.0839	14.19 ↑	0.0561	0.0486	15.51 ↑	0.0482	16.52 ↑	0.0453	24.03 ↑	1.18 ±0.21
	CNN_{3-4}	5,018	0.0747	0.0694	7.52 ↑	0.0693	7.72 ↑	0.0681	9.70 ↑	0.0465	0.0410	13.32 ↑	0.0409	13.59 ↑	0.0391	18.85 ↑	0.30 ±0.09
CIFAR10	9x100	910	0.0315	0.0211	49.03 ↑	0.0214	46.94 ↑	0.0192	63.58 ↑	0.0280	0.0183	52.70 ↑	0.0186	50.32 ↑	0.0133	110.07 ↑	4.92 ±0.01
	6x100	610	0.0221	0.0174	27.08 ↑	0.0176	26.14 ↑	0.0170	30.22 ↑	0.0165	0.0118	40.05 ↑	0.0120	37.82 ↑	0.0111	48.24 ↑	3.04 ±0.02
	5x100	510	0.0200	0.0167	19.76 ↑	0.0167	19.47 ↑	0.0163	22.40 ↑	0.0137	0.0104	31.80 ↑	0.0104	31.42 ↑	0.0099	38.45 ↑	2.44 ±0.01
	3x50	160	0.0206	0.0178	15.43 ↑	0.0179	14.66 ↑	0.0176	16.88 ↑	0.0144	0.0113	27.57 ↑	0.0115	25.24 ↑	0.0110	31.30 ↑	0.43 ±0.00
	4x100	410	0.0161	0.0140	15.23 ↑	0.0140	14.81 ↑	0.0138	16.56 ↑	0.0111	0.0089	24.61 ↑	0.0090	23.63 ↑	0.0087	27.62 ↑	1.85 ±0.01
	CNN_{3-4}	6,746	0.0187	0.0181	3.38 ↑	0.0181	3.32 ↑	0.0181	3.43 ↑	0.0109	0.0103	5.93 ↑	0.0103	5.83 ↑	0.0103	6.13 ↑	0.56 ±0.08
	CNN_{3-2}	3,378	0.0185	0.0180	2.49 ↑	0.0180	2.55 ↑	0.0180	2.67 ↑	0.0125	0.0120	4.34 ↑	0.0120	4.34 ↑	0.0120	4.60 ↑	0.30 ±0.06

range of visual recognition applications [22, 27, 30, 34, 43]; we also consider FNNs to expand the architecture variety. We trained all the networks on the image databases MNIST [23], Fashion MNIST [53], and CIFAR10 [21]. We chose the first 100 images from the test set of each dataset as in [5, 51, 55], among which only correctly-classified images by the neural network are considered in our experiments.

For each network architecture, we trained three variant neural networks using the Sigmoid, Tanh, and Arctan activation functions, respectively. In Experiment **I** the networks contain only non-negative weights. We used Adam or SGD optimizer with at least 50 epochs of batch size 128. The test set accuracy of networks trained on MNIST, Fashion MNIST, and CIFAR10 is around 0.9, 0.85, and 0.4, respectively. In Experiment **II** and **III** we trained 1-hidden-layer networks and used pre-trained models [2, 40, 51] (as in Table 1, Section 3.2) with no constraint on the weights. Note that the number of neurons in FNNs can be considerably fewer than that in CNNs [24], while the networks can still achieve up to 0.99 test accuracy.

Metrics. We use certified lower bound to assess *effectiveness*, and $(\epsilon' - \epsilon)/\epsilon$ to quantify the precision improvement, where ϵ' and ϵ denote the lower bounds certified by NeWise and each competing approach, respectively. We consider both *average* and *standard deviation* (SD) of certified lower bounds; in particular, SD is a suitable measure of sensitivity of the approximations to input images: A larger SD implies a better sensitivity [51]. For *efficiency*, we record the average computation time over the (correctly-classified) images.

Experimental Setup. All the experiments were conducted on a workstation running Ubuntu 18.04 with a 2.35GHz 32-core AMD EPYC 7452 CPU and 128 GB memory.

6.2 Experimental Results

Experiment I. Table 2 shows the comparison results for 22 Sigmoid models with non-negative weights. Regarding the precision of verification results, our NeWise computes significantly larger certified lower bounds than the competitors for *all* the models. In particular, for *average*, NeWise achieves up to 96.22% improvement, i.e., FNNs with 4 hidden layers trained on Fashion MNIST. NeWise improves the precision even more with *standard deviation* (up to 129.33%). This indicates that our approach is more sensitive to input images compared to the other approaches: The more the certified lower bound is improved, the larger deviation the network exhibits.

Regarding efficiency, all the approaches incur similar overhead as expected (they share the same complexity, i.e., $O(1)$ on each neuron). We use $p \pm q$ to denote their average time cost p and the size of the interval $2q$. Table 3 presents the results on the Tanh models. NeWise computes *even larger* certified lower bounds, e.g., with up to 251.28%. We omit the similar time overheads in Table 3. See Appendix C for the complete results, including those on the Arctan models.

All these experimental results provide strong independent validation of our mathematical proof of Theorem 2.

Experiment II. We evaluate the performance of Algorithm 1 on 1-hidden-layer networks. Table 4 shows the comparison results with the other three tools. We only show the metric of standard deviation due to space limit. As shown in the table, Algorithm 1 can compute larger bounds with up to 160.66% improvement. Complete results are available in the Appendix C .

Regarding efficiency, the searching algorithm needs more time because it is in polynomial time, unlike the constant-time approach for the non-negative models. Nevertheless, the gradient-decent-based approach has been proven an efficient and practical solution

Table 3: Performance comparison of NeWise (NW) with DeepCert (DC), VeriNet (VN), and RobustVerifier (RV) on non-negative Tanh networks. $t \times n$ refers to an FNN with t layers and n neurons per layer. CNN_{t-c} denotes a CNN with t layers and c filters of size 3×3.

Dataset	Model	Certified Lower Bound (Standard Deviation)						
		NW	DC	Impr. (%)	VN	Impr. (%)	RV	Impr. (%)
MNIST	5x100	0.0018	0.0005	233.96 ↑	0.0006	195.00 ↑	0.0006	216.07 ↑
	3x700	0.0027	0.0008	251.28 ↑	0.0009	191.49 ↑	0.0009	191.49 ↑
	3x400	0.0018	0.0007	166.67 ↑	0.0008	128.57 ↑	0.0007	137.84 ↑
	CNN_{6-5}	0.0243	0.0115	111.84 ↑	0.0131	85.94 ↑	0.0087	179.13 ↑
	3x50	0.0012	0.0009	29.79 ↑	0.0010	27.08 ↑	0.0008	45.24 ↑
	CNN_{3-4}	0.0067	0.0055	21.05 ↑	0.0058	14.80 ↑	0.0055	20.83 ↑
	CNN_{5-5}	0.0108	0.0090	20.24 ↑	0.0092	17.50 ↑	0.0087	24.54 ↑
	CNN_{4-5}	0.0074	0.0061	21.21 ↑	0.0063	17.19 ↑	0.0060	23.63 ↑
Fashion MNIST	3x100	0.0156	0.0105	48.81 ↑	0.0110	42.04 ↑	0.0091	70.79 ↑
	CNN_{4-5}	0.0188	0.0134	41.12 ↑	0.0139	35.83 ↑	0.0129	45.82 ↑
	CNN_{6-5}	0.0329	0.0237	38.83 ↑	0.0242	35.67 ↑	0.0180	82.66 ↑
	2x100	0.0109	0.0081	35.27 ↑	0.0085	28.59 ↑	0.0077	41.95 ↑
	2x200	0.0102	0.0076	33.38 ↑	0.0080	27.06 ↑	0.0076	33.55 ↑
	CNN_{5-5}	0.0201	0.0153	31.52 ↑	0.0158	27.03 ↑	0.0125	60.69 ↑
CIFAR10	3x200	0.0176	0.0083	113.30 ↑	0.0092	90.91 ↑	0.0080	119.40 ↑
	3x50	0.0111	0.0073	53.52 ↑	0.0077	44.73 ↑	0.0071	56.32 ↑
	3x100	0.0435	0.0243	78.79 ↑	0.0270	61.35 ↑	0.0256	69.66 ↑
	3x400	0.0441	0.0245	79.67 ↑	0.0291	51.58 ↑	0.0253	74.69 ↑
	CNN_{3-2}	0.0106	0.0102	4.01 ↑	0.0102	4.01 ↑	0.0102	4.21 ↑
	CNN_{3-4}	0.0062	0.0061	1.80 ↑	0.0061	1.80 ↑	0.0061	1.96 ↑
	CNN_{3-5}	0.0066	0.0065	1.86 ↑	0.0065	1.86 ↑	0.0065	2.02 ↑

to such convex optimization problems [17]. When the size of a network is reasonably small, such overhead is acceptable, compared with the improvement of the verification results.

Experiment III. Despite the infeasibility of network-wise tightest approximations in the general case (Section 3.3), we have explored the performance of our approximation method and the competitors on the networks of mixed weights. Table 5 shows the certified lower bounds returned by each approach for 11 CNNs and 9 FNNs.

First, the performance of each approach as compared with the others varies under different mixed-weight models. This coincides with our analysis in Section 3.3: Pure neuron-wise tightness does not imply a network-wise tightness. Moreover, we observe that our NeWise performs surprisingly better than other approaches on all the experimented CNNs, while DeepCert and VeriNet return larger certified lower bounds on the FNNs. The results evidenced network architecture is another factor influencing the verification. One possible reason is that a convolutional neural network is more possible to be monotonic based on the fact that the neurons' weights on the same layer are constrained to be identical [24].

Finally, we observe that average and standard deviation share the same increase/decrease trends. This indicates that a tighter approximation is more sensitive to the input images, which conforms to our conclusion in Experiment **I**.

6.3 Threats to Validity

We discuss potential threats to the validity of our approach in terms of its application domains.

Neural Networks with ReLU Activation Functions. Despite the focus on the Sigmoid-like activation functions, our approach is also applicable to the ReLU activation functions. A ReLU function $\sigma(x) = max(x, 0)$, with $x \in [l, u]$, only needs approximation when $l < 0$ and $u > 0$; the upper, resp. lower, linear bound would be then $y = \frac{u}{u-l}(x-l)$, resp. $y = 0$. Hence, the approximation is the tightest

Table 4: Performance comparison of Algorithm 1 with DeepCert (DC), VeriNet (VN), and RobustVerifier (RV) on 1-hidden-layer Sigmoid networks. $t \times n$ refers to an FNN with t layers and n neurons per layer. CNN_{t-c-f} denotes a CNN with t layers and c filters of size $f \times f$. $*$ and $+$ mark the models trained on MNIST and Fashion MNIST, respectively.

Arch.	Model	Certified Lower Bound (Standard Deviation)						
		Alg.1	DC	Impr. (%)	VN	Impr. (%)	RV	Impr. (%)
CNN	$\text{CNN}_{2-1-5}{}^{*}$	0.0358	0.0145	146.32 ↑	0.0143	150.98 ↑	0.0137	160.66↑
	$\text{CNN}_{2-2-5}{}^{*}$	0.0308	0.0208	47.82 ↑	0.0207	48.96 ↑	0.0187	64.23↑
	$\text{CNN}_{2-3-5}{}^{*}$	0.0305	0.0197	54.80 ↑	0.0196	55.28 ↑	0.0176	73.57↑
	$\text{CNN}_{2-4-5}{}^{*}$	0.0419	0.0233	79.70 ↑	0.0232	80.56 ↑	0.0210	99.40↑
	$\text{CNN}_{2-5-3}{}^{*}$	0.0319	0.0182	75.22 ↑	0.0182	75.89 ↑	0.0176	81.59↑
	$\text{CNN}_{2-1-5}{}^{+}$	0.0497	0.0385	29.08 ↑	0.0386	28.74 ↑	0.0348	42.52↑
	$\text{CNN}_{2-2-5}{}^{+}$	0.0547	0.0353	54.77 ↑	0.0355	53.94 ↑	0.0311	75.66↑
	$\text{CNN}_{2-3-5}{}^{+}$	0.0541	0.0371	45.76 ↑	0.0374	44.71 ↑	0.0344	57.28↑
	$\text{CNN}_{2-4-5}{}^{+}$	0.0540	0.0366	47.48 ↑	0.0367	47.00 ↑	0.0336	60.41↑
	$\text{CNN}_{2-5-3}{}^{+}$	0.0598	0.0340	75.97 ↑	0.0340	75.71 ↑	0.0312	91.34↑
FNN	1x50 $*$	0.0122	0.0082	49.16 ↑	0.0085	43.89 ↑	0.0062	96.32 ↑
	1x100$*$	0.0107	0.0064	67.67 ↑	0.0066	61.10 ↑	0.0050	114.80 ↑
	1x150$*$	0.0124	0.0083	50.17 ↑	0.0085	45.59 ↑	0.0064	93.75 ↑
	1x200$*$	0.0127	0.0074	71.99 ↑	0.0076	68.35 ↑	0.0058	120.58 ↑
	1x250$*$	0.0120	0.0075	60.93 ↑	0.0076	58.37 ↑	0.0060	100.82 ↑
	1x50 $^{+}$	0.0184	0.0117	56.83 ↑	0.0122	51.04 ↑	0.0089	107.35 ↑
	1x100^{+}	0.0149	0.0119	25.06 ↑	0.0123	21.89 ↑	0.0088	70.46 ↑
	1x150^{+}	0.0183	0.0120	52.83 ↑	0.0123	49.35 ↑	0.0090	103.61 ↑
	1x200^{+}	0.0216	0.0129	67.41 ↑	0.0132	63.74 ↑	0.0096	125.31 ↑
	1x250^{+}	0.0170	0.0126	34.67 ↑	0.0128	32.88 ↑	0.0095	77.96 ↑

for non-negative neural networks. However, linear approximation is not a necessity for ReLU due to its piece-wise linearity. There are more precise (both sound and complete) verification approaches (by using, e.g., SMT [20] and Mixed Integer Linear Programming [6]) which could compute larger certified lower bounds.

FNNs with Mixed Weights. For such networks, it is generally unpredictable which approach would compute the most precise verification result (despite a 10% decrease on average in our approach). To the best of our knowledge, the only feasible way to examine a proposed approximation under non-trivial FNNs is by empirical analysis. Tackling this fundamentally and efficiently remains to be an open research problem.

7 RELATED WORK

This work is a sequel to many pioneering efforts, which we classify into the following three categories.

Linear Approximations of Sigmoid-like activation functions. NeVer [33] uses piece-wise linear constraints for approximation and is therefore unscalable. Both CROWN [55] and CNN-Cert [5] consider the tangent line at the midpoint of $[l, u]$ as one of the linear bounds. DeepCert [51] defines a fine-grained approximation strategy by calculating the slopes of the two linear constraints according to l and u. RobustVerifier [26] leverages Taylor expansion at the midpoint of $[l, u]$. These approximations are intuitive but lack rigorous justifications or proofs for their better performance.

Lyu *et al.* [28] characterized the tightness of approximations in terms of the overestimation of output range of each hidden neuron. But they observed and admitted that by their definition tighter bounding lines do not ensure more precise results. By our definition, we show that in the case of one hidden layer, their definition also guarantees to be network-wise tightest. They proposed a gradient-based searching algorithm for near-tightest approximations under

Table 5: Performance comparison with DeepCert (DC), VeriNet (VN), and RobustVerifier (RV) on mixed-weights Sigmoid networks. ∗, +, and # mark the models trained on MNIST, Fashion MNIST, and CIFAR10, respectively.

Arch.	Model	#Neur.	Certified Lower Bound														Time (s)
			Average							Standard Deviation							
			NW	DC	Impr. (%)	VN	Impr. (%)	RV	Impr. (%)	NW	DC	Impr. (%)	VN	Impr. (%)	RV	Impr. (%)	
CNN	CNN_{3_2}*	2,514	0.0607	0.0579	4.92 ↑	0.0580	4.67 ↑	0.0569	6.82 ↑	0.0219	0.0202	8.06 ↑	0.0204	7.37 ↑	0.0192	13.79 ↑	0.17 ±0.04
	CNN_{3_4}*	5,018	0.0478	0.0472	1.17 ↑	0.0472	1.29 ↑	0.0464	2.95 ↑	0.0155	0.0153	1.11 ↑	0.0153	1.44 ↑	0.0146	5.87 ↑	0.31 ±0.08
	CNN_{4_5}*	8,680	0.0570	0.0539	5.64 ↑	0.0543	5.03 ↑	0.0522	9.16 ↑	0.0157	0.0145	8.64 ↑	0.0146	7.52 ↑	0.0132	19.45 ↑	1.18 ±0.20
	CNN_{5_5}*	10,680	0.0581	0.0548	6.06 ↑	0.0550	5.63 ↑	0.0512	13.42 ↑	0.0157	0.0142	10.48 ↑	0.0144	8.80 ↑	0.0120	30.81 ↑	2.99 ±0.38
	CNN_{6_5}*	12,300	0.0624	0.0590	5.71 ↑	0.0588	6.00 ↑	0.0541	15.27 ↑	0.0171	0.0153	12.03 ↑	0.0153	11.96 ↑	0.0123	39.72 ↑	5.72 ±0.46
	CNN_{8_5}*	14,570	0.1191	0.0878	35.58 ↑	0.0882	35.02 ↑	0.0685	73.75 ↑	0.0361	0.0248	45.60 ↑	0.0255	41.66 ↑	0.0163	122.22 ↑	15.27 ±0.78
	CNN_{4_5}+	8,680	0.0747	0.0720	3.73 ↑	0.0720	3.79 ↑	0.0666	12.16 ↑	0.0413	0.0376	9.85 ↑	0.0378	9.12 ↑	0.0313	31.73 ↑	1.19 ±0.21
	CNN_{5_5}+	10,680	0.0704	0.0676	4.14 ↑	0.0676	4.14 ↑	0.0605	16.51 ↑	0.0347	0.0318	9.03 ↑	0.0320	8.41 ↑	0.0244	41.82 ↑	2.99 ±0.40
	CNN_{6_5}+	12,300	0.0735	0.0695	5.77 ↑	0.0691	6.37 ↑	0.0626	17.32 ↑	0.0368	0.0341	7.97 ↑	0.0340	8.35 ↑	0.0278	32.57 ↑	5.81 ±0.55
	CNN_{3_2}#	3,378	0.0314	0.0312	0.58 ↑	0.0312	0.61 ↑	0.0311	1.06 ↑	0.0172	0.0169	1.65 ↑	0.0169	1.84 ↑	0.0168	2.69 ↑	0.31 ±0.06
	CNN_{6_5}#	17,110	0.0229	0.0224	2.19 ↑	0.0223	2.46 ↑	0.0212	7.77 ↑	0.0158	0.0153	3.20 ↑	0.0153	3.20 ↑	0.0141	12.13 ↑	10.31 ±0.68
FNN	3x50 *	160	0.0069	0.0076	-8.82 ↓	0.0077	-9.77 ↓	0.0065	6.62 ↑	0.0025	0.0027	-6.37 ↓	0.0028	-9.42 ↓	0.0021	18.48 ↑	0.14 ±0.00
	3x100*	310	0.0078	0.0086	-9.44 ↓	0.0087	-10.79↓	0.0074	4.44 ↑	0.0026	0.0029	-10.14 ↓	0.0029	-12.88 ↓	0.0023	10.30 ↑	2.14 ±0.03
	3x200*	610	0.0080	0.0091	-11.69↓	0.0091	-12.36↓	0.0079	1.01 ↑	0.0026	0.0030	-14.14 ↓	0.0031	-16.39 ↓	0.0024	5.37 ↑	10.77 ±0.01
	5x100*	510	0.0057	0.0061	-5.27 ↓	0.0062	-6.66 ↓	0.0052	10.79 ↑	0.0024	0.0025	-5.98 ↓	0.0026	-8.88 ↓	0.0021	12.38 ↑	4.38 ±0.03
	6x500*	3,010	0.0685	0.0778	-11.95↓	0.0776	-11.73↓	0.0665	3.05 ↑	0.0186	0.0210	-11.56 ↓	0.0210	-11.69 ↓	0.0152	21.98 ↑	154.39 ±0.36
	3x50 +	160	0.0092	0.0101	-9.67 ↓	0.0102	-10.29↓	0.0086	6.64 ↑	0.0035	0.0037	-6.74 ↓	0.0038	-9.90 ↓	0.0030	15.72 ↑	0.14 ±0.00
	5x100+	510	0.0071	0.0078	-8.51 ↓	0.0079	-10.01↓	0.0066	8.23 ↑	0.0036	0.0040	-8.79 ↓	0.0041	-11.68 ↓	0.0033	11.35 ↑	4.44 ±0.03
	3x50 #	160	0.0041	0.0045	-10.57↓	0.0045	-10.18↓	0.0042	-2.17 ↓	0.0018	0.0021	-14.90 ↓	0.0021	-14.49 ↓	0.0017	2.91 ↑	0.43 ±0.00
	5x100#	510	0.0033	0.0037	-10.60↓	0.0037	-10.60↓	0.0033	-0.60 ↓	0.0014	0.0017	-15.06 ↓	0.0016	-14.55 ↓	0.0013	5.22 ↑	2.45 ±0.01

their definition. However, the algorithm has been shown difficult to scale up to large-size networks because it needs to perform on every neuron, compared with other existing constant-time approaches [18, 51]. Our work is, to the best of our knowledge, the first provably tightest, constant-time linear approximation.

Defining Tightness for Linear Approximations. There has been a shift of focus from individual neurons to multiple neurons w.r.t. defining tightness for linear approximations, but most of the work only concerns about the ReLU networks. Tjandraatmadja *et al.* [41] experimentally show that the success of approximations hinges on how closely they approximate the object that they are relaxing. Salman *et al.* [36] reveal an inherent barrier of the approximation-based approaches for the ReLU networks and require for the tightest pre-activation upper and lower bounds of all the neurons in networks. Singh *et al.* [38] approximate multiple neurons simultaneously to obtain the tighter bounds. In contrast to this line of research, we have defined both neuron-wise and network-wise tightness to characterize linear approximations of Sigmoid-like activation functions.

Other Robustness Verification Approaches. In addition to approximation, other techniques have also been used for the robustness verification of neural networks. Abstract interpretation [11], a technique that was originally proposed for program verification, has been proven both effective and efficient in neural network verification [16, 39, 40]. These approaches also rely on over-approximation but to transform the original verification problem into dedicated abstract domains. We believe that our approximation approach is also applicable to produce more precise verification results for non-negative neural networks. Other verification methods leverage the Lipschitz continuity feature of neural networks to estimate the output ranges [10, 25, 35]. Although the approximation to an activation function can be bypassed using the Lipschitz constant, it would still be helpful to compute tighter Lipschitz constants by estimating the input range of the activation function via the approximation.

8 CONCLUDING REMARKS

We have presented *network-wise tightness*, a novel and unified characterization of the tightness of linear approximations in robustness verification of Sigmoid-like neural networks. We have shown that (i) to achieve precise verification results, activation functions in a network should *not* be approximated with the same existing neuron-wise tightness criterion; (ii) computing the network-wise tightest approximation is computationally expensive and impractical due to its non-convexity; and (iii) how to bypass the complexity barrier via a neuron-wise tightest approximation. The experimental results demonstrate that our approximation approach outperforms state-of-the-art approaches under three scenarios, i.e., non-negative networks, 1-hidden-layer networks, and convolutional networks.

Our work sheds light on the pursuit of robust neural networks via tightening linear approximations. The ineffectiveness of neuron-wise tightness on general networks calls for new, potentially hybrid, approximation strategies. The intrinsic high complexity in computing the network-wise tightest approximation motivates us to rethink of both fundamental and the heuristic trade-offs between precision and efficiency in neural network verification. For mixed-weight neural networks, there may be latent factors that could influence the tightness of approximations. One promising direction is to explore possible combinations of existing tightness characterizations to achieve network-wise tightness while taking into account the features of weight distributions and network architectures.

ACKNOWLEDGMENTS

The authors thank the reviewers for their constructive comments. This work was supported in part by the National Key Research and Development (2019YFA0706404), the National Nature Science Foundation of China (61972150), the NSFC-ISF Joint Program (62161146001, 3420/21), the Fundamental Research Funds for Central Universities, and the Opening Project of Shanghai Trusted Industrial Control Platform. Jing Liu and Min Zhang are the corresponding authors.

REFERENCES

[1] Afan Ali and Fan Yangyu. 2017. Automatic modulation classification using deep learning based on sparse autoencoders with nonnegativity constraints. *IEEE signal processing letters* 24, 11 (2017), 1626–1630.

[2] aptx4869tjx. 2021. Pretrained Models. https://github.com/aptx4869tjx/train_network.

[3] Christel Baier and Joost-Pieter Katoen. 2008. *Principles of model checking*. MIT press.

[4] Teodora Baluta, Zheng Leong Chua, Kuldeep S. Meel, and Prateek Saxena. 2021. Scalable Quantitative Verification For Deep Neural Networks. In *43rd IEEE/ACM International Conference on Software Engineering, ICSE 2021, Madrid, Spain, 22-30 May 2021*. IEEE, 312–323.

[5] Akhilan Boopathy, Tsui-Wei Weng, Pin-Yu Chen, Sijia Liu, and Luca Daniel. 2019. CNN-Cert: An Efficient Framework for Certifying Robustness of Convolutional Neural Networks. In *AAAI Conference on Artificial Intelligence (AAAI)*. 3240–3247.

[6] Elena Botoeva, Panagiotis Kouvaros, Jan Kronqvist, Alessio Lomuscio, and Ruth Misener. 2020. Efficient Verification of ReLU-Based Neural Networks via Dependency Analysis. In *AAAI Conference on Artificial Intelligence (AAAI)*. AAAI Press, 3291–3299.

[7] Nicholas Carlini and David Wagner. 2017. Towards evaluating the robustness of neural networks. In *IEEE symposium on security and privacy (S&P)*. IEEE, 39–57.

[8] Fabrício Ceschin, Marcus Botacin, Heitor Murilo Gomes, Luiz S Oliveira, and André Grégio. 2019. Shallow security: On the creation of adversarial variants to evade machine learning-based malware detectors. In *Proceedings of the 3rd Reversing and Offensive-oriented Trends Symposium*. 1–9.

[9] Edmund M Clarke. 1997. Model checking. In *International Conference on Foundations of Software Technology and Theoretical Computer Science*. Springer, 54–56.

[10] Patrick L Combettes and Jean-Christophe Pesquet. 2020. Lipschitz certificates for layered network structures driven by averaged activation operators. *SIAM Journal on Mathematics of Data Science* 2, 2 (2020), 529–557.

[11] Patrick Cousot and Radhia Cousot. 1977. Abstract interpretation: a unified lattice model for static analysis of programs by construction or approximation of fixpoints. In *ACM Symposium on Principles of Programming Languages (POPL)*. 238–252.

[12] Isaac Dunn, Hadrien Pouget, Daniel Kroening, and Tom Melham. 2021. Exposing previously undetectable faults in deep neural networks. In *30th ACM SIGSOFT International Symposium on Software Testing and Analysis (ISSTA)*. ACM, 56–66.

[13] Souradeep Dutta, Susmit Jha, Sriram Sankaranarayanan, and Ashish Tiwari. 2018. Output Range Analysis for Deep Feedforward Neural Networks. In *NASA Formal Methods Symposium (NFM)*. Springer, 121–138.

[14] Ruediger Ehlers. 2017. Formal verification of piece-wise linear feed-forward neural networks. In *International Symposium on Automated Technology for Verification and Analysis*. Springer, 269–286.

[15] William Fleshman, Edward Raff, Jared Sylvester, et al. 2018. Non-Negative Networks Against Adversarial Attacks. *CoRR* abs/1806.06108 (2018). http://arxiv.org/abs/1806.06108

[16] Timon Gehr, Matthew Mirman, Dana Drachsler-Cohen, Petar Tsankov, Swarat Chaudhuri, and Martin Vechev. 2018. AI2: Safety and Robustness Certification of Neural Networks with Abstract Interpretation. In *IEEE Symposium on Security and Privacy (S&P)*. IEEE, 3–18.

[17] Saad Hikmat Haji and Adnan Mohsin Abdulazeez. 2021. Comparison of optimization techniques based on gradient descent algorithm: A review. *PalArch's Journal of Archaeology of Egypt/Egyptology* 18, 4 (2021), 2715–2743.

[18] Patrick Henriksen and Alessio R. Lomuscio. 2020. Efficient Neural Network Verification via Adaptive Refinement and Adversarial Search. In *European Conference on Artificial Intelligence (ECAI)*. IOS Press, 2513–2520.

[19] Omid Kargarnovin, Amir Mahdi Sadeghzadeh, and Rasool Jalili. 2021. Mal2GCN: A Robust Malware Detection Approach Using Deep Graph Convolutional Networks With Non-Negative Weights. *arXiv preprint arXiv:2108.12473* (2021).

[20] Guy Katz, Clark Barrett, David L Dill, Kyle Julian, and Mykel J Kochenderfer. 2017. Reluplex: An Efficient SMT Solver for Verifying Deep Neural Networks. In *International Conference on Computer Aided Verification (CAV)*. Springer, 97–117.

[21] Alex Krizhevsky, Geoffrey Hinton, et al. 2009. Learning Multiple Layers of Features from Tiny Images. (2009).

[22] Alex Krizhevsky, Ilya Sutskever, and Geoffrey E. Hinton. 2017. ImageNet classification with deep convolutional neural networks. *Commun. ACM* 60, 6 (2017), 84–90.

[23] Yann LeCun, Léon Bottou, Yoshua Bengio, and Patrick Haffner. 1998. Gradient-Based Learning Applied to Document Recognition. *Proc. IEEE* 86, 11 (1998), 2278–2324.

[24] Yann LeCun, Léon Bottou, Yoshua Bengio, and Patrick Haffner. 1998. Gradient-based learning applied to document recognition. *Proc. IEEE* 86, 11 (1998), 2278–2324.

[25] Sungyoon Lee, Jaewook Lee, and Saerom Park. 2020. Lipschitz-certifiable training with a tight outer bound. *Annual Conference on Neural Information Processing Systems (NeurIPS)* 33 (2020), 16891–16902.

[26] Wang Lin, Zhengfeng Yang, Xin Chen, Qingye Zhao, Xiangkun Li, Zhiming Liu, and Jifeng He. 2019. Robustness Verification of Classification Deep Neural Networks via Linear Programming. In *IEEE/CVF Conference on Computer Vision and Pattern Recognition (CVPR)*. 11418–11427.

[27] Jonathan Long, Evan Shelhamer, and Trevor Darrell. 2015. Fully convolutional networks for semantic segmentation. In *IEEE/CVF Conference on Computer Vision and Pattern Recognition (CVPR)*. IEEE Computer Society, 3431–3440.

[28] Zhaoyang Lyu, Ching-Yun Ko, Zhifeng Kong, Ngai Wong, Dahua Lin, and Luca Daniel. 2020. Fastened CROWN: Tightened Neural Network Robustness Certificates. In *AAAI Conference on Artificial Intelligence (AAAI)*. 5037–5044.

[29] Ana Neacsu, Jean-Christophe Pesquet, and Corneliu Burileanu. 2020. Accuracy-Robustness Trade-Off for Positively Weighted Neural Networks. In *International Conference on Acoustics, Speech and Signal Processing (ICASSP)*. IEEE, 8389–8393.

[30] Tianxiang Pan, Bin Wang, Guiguang Ding, and Jun-Hai Yong. 2017. Fully Convolutional Neural Networks with Full-Scale-Features for Semantic Segmentation. In *AAAI Conference on Artificial Intelligence (AAAI)*. AAAI Press, 4240–4246.

[31] Harsh Nilesh Pathak and Randy Clinton Paffenroth. 2020. Non-convex Optimization Using Parameter Continuation Methods for Deep Neural Networks. *Deep Learning Applications, Volume 2* 1232 (2020), 273–298.

[32] Brandon Paulsen, Jingbo Wang, Jiawei Wang, and Chao Wang. 2020. NEUROD-IFF: Scalable Differential Verification of Neural Networks using Fine-Grained Approximation. In *International Conference on Automated Software Engineering (ASE)*. IEEE, 784–796.

[33] Luca Pulina and Armando Tacchella. 2010. An Abstraction-Refinement Approach to Verification of Artificial Neural Networks. In *International Conference on Computer Aided Verification (CAV)*. Springer, 243–257.

[34] Shaoqing Ren, Kaiming He, Ross B. Girshick, and Jian Sun. 2017. Faster R-CNN: Towards Real-Time Object Detection with Region Proposal Networks. *IEEE Transactions on Pattern Analysis and Machine Intelligence* 39, 6 (2017), 1137–1149.

[35] Wenjie Ruan, Xiaowei Huang, and Marta Kwiatkowska. 2018. Reachability analysis of deep neural networks with provable guarantees. In *International Joint Conference on Artificial Intelligence(IJCAI)*. 2651–2659.

[36] Hadi Salman, Greg Yang, Huan Zhang, Cho-Jui Hsieh, and Pengchuan Zhang. 2019. A Convex Relaxation Barrier to Tight Robustness Verification of Neural Networks. In *Annual Conference on Neural Information Processing Systems (NeurIPS)*. 9832–9842.

[37] Marco Sälzer and Martin Lange. 2021. Reachability Is NP-Complete Even for the Simplest Neural Networks. *CoRR* abs/2108.13179 (2021).

[38] Gagandeep Singh, Rupanshu Ganvir, Markus Püschel, and Martin T. Vechev. 2019. Beyond the Single Neuron Convex Barrier for Neural Network Certification. In *Annual Conference on Neural Information Processing Systems (NeurIPS)*. 15072–15083.

[39] Gagandeep Singh, Timon Gehr, Matthew Mirman, Markus Püschel, and Martin T Vechev. 2018. Fast and Effective Robustness Certification.. In *Advances in Neural Information Processing Systems (NeurIPS)*. 10825–10836.

[40] Gagandeep Singh, Timon Gehr, Markus Püschel, and Martin Vechev. 2019. An Abstract Domain for Certifying Neural Networks. *Proceedings of the ACM on Programming Languages (POPL)* (2019), 1–30.

[41] Christian Tjandraatmadja, Ross Anderson, Joey Huchette, Will Ma, Krunal Patel, and Juan Pablo Vielma. 2020. The Convex Relaxation Barrier, Revisited: Tightened Single-Neuron Relaxations for Neural Network Verification. In *Annual Conference on Neural Information Processing Systems (NeurIPS)*.

[42] Vincent Tjeng, Kai Xiao, and Russ Tedrake. 2019. Evaluating Robustness of Neural Networks with Mixed Integer Programming. In *International Conference on Learning Representations (ICLR)*.

[43] Alexander Toshev and Christian Szegedy. 2014. DeepPose: Human Pose Estimation via Deep Neural Networks. In *IEEE/CVF Conference on Computer Vision and Pattern Recognition (CVPR)*. IEEE Computer Society, 1653–1660.

[44] Hoang-Dung Tran, Xiaodong Yang, Diego Manzanas Lopez, Patrick Musau, Luan Viet Nguyen, Weiming Xiang, Stanley Bak, and Taylor T Johnson. 2020. NNV: the neural network verification tool for deep neural networks and learning-enabled cyber-physical systems. In *International Conference on Computer Aided Verification(CAV)*. Springer, 3–17.

[45] Shiqi Wang, Kexin Pei, Justin Whitehouse, Junfeng Yang, and Suman Jana. 2018. Efficient formal safety analysis of neural networks. In *Annual Conference on Neural Information Processing Systems (NeurIPS)*. 6369–6379.

[46] Shiqi Wang, Kexin Pei, Justin Whitehouse, Junfeng Yang, and Suman Jana. 2018. Formal Security Analysis of Neural Networks using Symbolic Intervals. In *USENIX Security Symposium (USENIX Security)*. 1599–1614.

[47] Shiqi Wang, Huan Zhang, Kaidi Xu, Xue Lin, Suman Jana, Cho-Jui Hsieh, and J Zico Kolter. 2021. Beta-crown: Efficient bound propagation with per-neuron split constraints for neural network robustness verification. *Annual Conference on Neural Information Processing Systems (NeurIPS)* 34 (2021).

[48] Lily Weng, Huan Zhang, Hongge Chen, Zhao Song, et al. 2018. Towards Fast Computation of Certified Robustness for ReLU Networks. In *International Conference on Machine Learning (ICML)*. PMLR, 5276–5285.

[49] Tsui-Wei Weng, Huan Zhang, Hongge Chen, Zhao Song, et al. 2018. Towards Fast Computation of Certified Robustness for ReLU Networks. In *International*

Conference on Machine LearningICML, Vol. 80. PMLR, 5273–5282.
[50] Jeannette M Wing. 2021. Trustworthy AI. *Commun. ACM* 64, 10 (2021), 64–71.
[51] Yiting Wu and Min Zhang. 2021. Tightening Robustness Verification of Convolutional Neural Networks with Fine-Grained Linear Approximation. In *AAAI Conference on Artificial Intelligence (AAAI)*. 11674–11681.
[52] Weiming Xiang, Hoang-Dung Tran, and Taylor T Johnson. 2018. Output reachable set estimation and verification for multilayer neural networks. *IEEE transactions on neural networks and learning systems* 29, 11 (2018), 5777–5783.
[53] Han Xiao, Kashif Rasul, and Roland Vollgraf. 2017. Fashion-MNIST: a Novel Image Dataset for Benchmarking Machine Learning Algorithms. *CoRR* abs/1708.07747 (2017).
[54] Ming Yan, Junjie Chen, Xiangyu Zhang, Lin Tan, Gan Wang, and Zan Wang. 2021. Exposing numerical bugs in deep learning via gradient back-propagation. In *29th ACM Joint European Software Engineering Conference and Symposium on the Foundations of Software Engineering (ESEC/FSE)*. ACM, 627–638.
[55] Huan Zhang, Tsui-Wei Weng, Pin-Yu Chen, Cho-Jui Hsieh, and Luca Daniel. 2018. Efficient Neural Network Robustness Certification with General Activation Functions. In *Annual Conference on Neural Information Processing Systems (NeurIPS)*. 4944–4953.

A A COUNTEREXAMPLE FOR ARCTAN

This section shows a counterexample for Arctan, where a tighter linear bound line for the activation function actually produces a less precise verification result.

The counterexample is shown in Figure 7. For simplicity, weights of edges are integers and biases are ignored. Let x_1 and x_2 represent the possible input values in $[-2,-1]$ and $[-1,0]$, respectively. In the output layer, if the value of x_5 is always greater than the one of x_6, we can claim that all x_1 in $[-2,-1]$ and x_2 in $[-1,0]$ are classified to the label of x_5. We introduce an auxiliary node x_7 to represent $x_5 - x_6$.

The two linear approximations in Figure 7 (a) and (b) share the same upper bounds. The lower bounds of x_3, x_4 (the red in (a)) are closer to the Arctan function than the ones (the blue in (b)). However, the output range $[-2.496, -1.572]$ of x_7 computed by the right approximation is more precise than $[-2.614, -1.572]$ computed by the left approximation.

B PROOF OF THEOREM 2

For k-layer neural network $f : \mathbb{R}^n \to \mathbb{R}^m$ satisfying the conditions in Theorem 2, we continue to use the symbol definition proposed. We assume that the upper and lower bounds of $\phi_r^t(x)$ are u_r^t and l_r^t, *i.e.*, $l_r^t \le \phi_r^t(x) \le u_r^t$. We consider the linear approximation of $\sigma(\phi_r^t(x))$ between $[l_r^t, u_r^t]$, where $\sigma(x)$ is a Sigmoid-like function. According to Definition 4, we denote the upper and lower linear bounds of $\sigma(\phi_r^t(x))$ obtained by our approach as $h_{U,r}^t(x)$ and $h_{L,r}^t(x)$, respectively.

First, we prove Lemma 1, i.e., the two conditions in the Theorem 2 guarantee that the network is monotonous.

Proof. For any selected item of input x_i, items in the i-th column of W^1 are all positive or all negative. Suppose that they are all positive, which means $\forall r \in \mathbb{Z}, 1 \le r \le n^1, w_{r,i}^1 > 0$. First we consider $t = 1$, for any value $x_i' > x_i''$ of x_i, $\phi_r^1(x_i') = w_{r,i}^1 x_i' > w_{r,i}^1 x_i'' = \phi_r^1(x_i'')$.
Suppose that for any $t \le T, 1 \le T$, $\phi_r^t(x_i') > \phi_r^t(x_i'')$ holds. Then we consider layer $T+1$, Since σ is monotonously increasing, and all items in W^{T+1} are non-negative, we have:

$$\phi_r^{T+1}(x_i') = \sum_p w_{r,p}^{T+1} \sigma(\phi_p^T(x_i')) \tag{13}$$

$$> \sum_p w_{r,p}^{T+1} \sigma(\phi_p^T(x_i'')) \tag{14}$$

$$= \phi_r^{T+1}(x_i'') \tag{15}$$

In summary, by mathematical induction, $\forall r, t, \phi_r^t(x_i)$ is monotonously increasing.

Similarly, if the items in the i-th column of W^1 are all negative, we can deduce that $\forall r, t, \phi_r^t(x_i)$ is monotonously decreasing. The network satisfies Definition 5. □

Lemma 2. *Given a k-layer neural network f satisfying Definition 5 and its input $x = [x_1, ..., x_n]$, $\forall t \in \mathbb{Z}, 1 \le t \le k$, the j-th item in layer $t+1$ satisfies:*

$$\min_{x \in \mathbb{B}_\infty(x_0,\epsilon)} \phi_j^{t+1}(x) = \sum_r w_{j,r}^{t+1} \min_{x \in \mathbb{B}_\infty(x_0,\epsilon)} \sigma(\phi_r^t(x))$$

Proof. Suppose that f is network-wise monotonously increasing. $\forall$ selected i, from Definition 5, $\forall t$, $\phi_r^t(x_i)$ and $\phi_r^{t+1}(x_i)$ are both monotonously increasing. Suppose that $x_i \in [l_i^0, u_i^0]$, $x_{min} := [l_1^0, ..., l_n^0]$, $x_{max} := [u_1^0, ..., u_n^0]$, then:

$$\begin{aligned}
\min_{x \in \mathbb{B}_\infty(x_0,\epsilon)} \phi_j^{t+1}(x) &= \phi_j^{t+1}(x_{min}) \\
&= \sum_r w_{j,r}^{t+1} \sigma(\phi_r^t(x_{min})) \\
&= \sum_r w_{j,r}^{t+1} \sigma(\min_{x \in \mathbb{B}_\infty(x_0,\epsilon)} \phi_r^t(x)) \\
&= \sum_r w_{j,r}^{t+1} \min_{x \in \mathbb{B}_\infty(x_0,\epsilon)} \sigma(\phi_r^t(x))
\end{aligned}$$ □

Next, we prove the optimality of our approximation approach from the perspective of a single neuron.

Lemma 3. *Given function $f : \mathbb{R}^n \to \mathbb{R}$, let f's definition domain be D and its range be $[l, u]$, if the definition domain of function $g : \mathbb{R} \to \mathbb{R}$ is $[l, u]$, we can define compound function $g \circ f : \mathbb{R}^n \to \mathbb{R}$. Suppose that g is a monotonically increasing function, then we have:*

$$\min_{x \in D} g \circ f(x) = g(l), \quad \max_{x \in D} g \circ f(x) = g(u).$$

Proof. Because g is monotonically increasing, there is $\forall x \in [l, u], g(l) \le g(x) \le g(u)$. Then

$$\begin{aligned}
&\min_{x \in D} g \circ f(x) = g(\min_{x \in D} f(x)) = g(l), \text{and,} \\
&\max_{x \in D} g \circ f(x) = g(\max_{x \in D} f(x)) = g(u)
\end{aligned}$$ □

Theorem 3. *Given a neural network f, let $\phi^t : \mathbb{R}^n \to \mathbb{R}^{n^t}$ be the compound function of the first t layers of f. The r-th row of ϕ^t can be denoted as $\phi_r^t : \mathbb{R}^n \to \mathbb{R}$. When the input x is bounded in a norm-ball $\mathbb{B}_\infty(x_0, \epsilon)$, ϕ_r^t ranges in $[l_r^t, u_r^t]$, which is the definition domain of $h_{U,r}^t$ and $h_{L,r}^t$. We have:*

$$\min_{x \in \mathbb{B}_\infty(x_0,\epsilon)} h_{L,r}^t \circ \phi_r^t(x) = h_{L,r}^t(l_r^t), \text{and,}$$
$$\max_{x \in \mathbb{B}_\infty(x_0,\epsilon)} h_{U,r}^t \circ \phi_r^t(x) = h_{U,r}^t(u_r^t).$$

Proof. According to Definition 4, $h_{U,r}^t(x) = \alpha_{U,r}^t x + \beta_{U,r}^t$, $h_{L,r}^t(x) = \alpha_{L,r}^t x + \beta_{L,r}^t$. In our approximation, $h_{L,r}^t$ and $h_{L,r}^t$ are always monotonically increasing. By replacing f and g in Lemma 3 with ϕ_r^t and $h_{L,r}^t$ (*resp.* $h_{U,r}^t$), we can easily get the conclusion. □

Theorem 3 says that our approximation method does not overestimate the output range of current neuron. That is because $h_{L,r}^t(l_r^t) = \sigma(l_r^t)$ and $h_{U,r}^t(u_r^t) = \sigma(u_r^t)$. That is, the output range of $\sigma(\phi_r^t(x))$ after the linear approximation is still $[\sigma(l_r^t), \sigma(u_r^t)]$.

When dealing with the lower bound of $\phi_j^{t+1}(x)$ - j-th output of layer $t+1$ under the condition that $x \in \mathbb{B}_\infty(x_0, \epsilon)$, we have:

$$\min_{x \in \mathbb{B}_\infty(x_0,\epsilon)} \phi_j^{t+1}(x) = \sum_r w_{j,r}^{t+1} \min_{x \in \mathbb{B}_\infty(x_0,\epsilon)} \sigma(\phi_r^t(x)) \tag{16}$$

$$= \sum_r w_{j,r}^{t+1} \min_{x \in \mathbb{B}_\infty(x_0,\epsilon)} h_{L,r}^t \circ \phi_r^t(x) \tag{17}$$

$$= \sum_r w_{j,r}^{t+1} h_{L,r}^t(l_r^t) \tag{18}$$

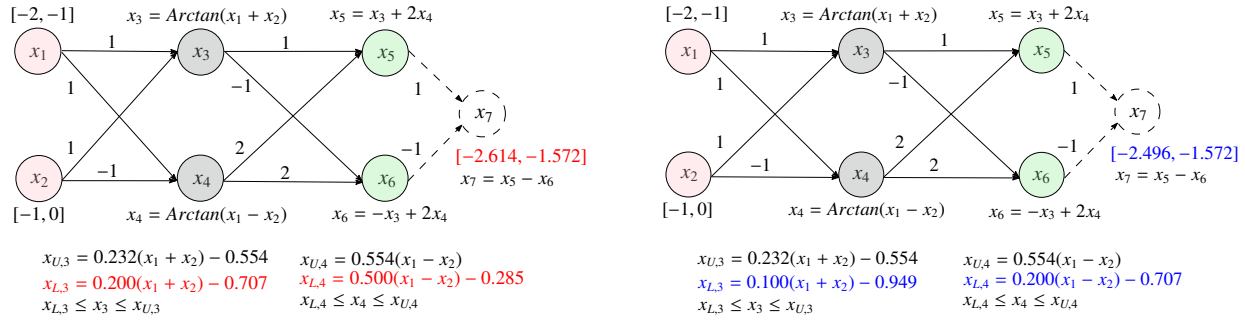

(a) Two lower bounds (red) closer to the Arctan function.

(b) Two lower bounds (blue) farther from the Arctan function.

Figure 7: Output ranges calculated by different linear approximations on the neural networks with Arctan.

where (16) is the conclusion of Lemma 2, and (18) is derived from (17) according to Theorem 3.

Likewise, we have:

$$\max_{x \in \mathbb{B}_\infty(x_0,\epsilon)} \phi_j^{t+1}(x) = \sum w_{j,r}^t h_{U,r}^t(u_r^t). \tag{19}$$

Theorem 4. *For networks satisfying conditions in Theorem 2, our linear approximation guarantees that (18) is the largest and (19) is the smallest among all possible approximations.*

Proof. Given an arbitrary other lower and upper linear bounds $\hat{h}_{L,r}^t$ and $\hat{h}_{U,r}^t$, there are $\hat{h}_{L,r}^t(x) \le \sigma(x)$ and $\hat{h}_{U,r}^t(x) \ge \sigma(x)$ for all $x \in [l_r^t, u_r^t]$, which implies that $\hat{h}_{L,r}^t(l_r^t) \le \sigma(l_r^t)$ and $\hat{h}_{U,r}^t(u_r^t) \ge \sigma(u_r^t)$. According to our linear approximation:

$$h_{L,r}^t(l_r^t) = \sigma(l_r^t) \ge \hat{h}_{L,r}^t(l_r^t), \text{and,}$$
$$h_{U,r}^t(u_r^t) = \sigma(u_r^t) \le \hat{h}_{U,r}^t(u_r^t).$$

As a result, for $w_{j,r}^t \ge 0$, we have the following formula hold:

$$\sum w_{j,r}^t h_{L,r}^t(l_r^t) \ge \sum w_{j,r}^t \hat{h}_{L,r}^t(l_r^t), \text{and,}$$
$$\sum w_{j,r}^t h_{U,r}^t(u_r^t) \le \sum w_{j,r}^t \hat{h}_{U,r}^t(u_r^t).$$

So our linear approximation obtains the supremum of (18) and the infimum of (19). □

According to Theorem 4, our approximation obtains the upper bound of $\min_{x \in \mathbb{B}_\infty(x_0,\epsilon)} \phi_j^{t+1}(x)$. Next, we prove the network-wise tightness of our approach through Definition 3. Let (f_L, f_U) be our linear approximation of f with f_U and f_L the upper and lower bounds, respectively. Suppose that there exists another linear approximation $(\hat{f}_L, \hat{f}_U)$ and label s s.t.

$$\min_{x \in \mathbb{B}_\infty(x_0,\epsilon)} f_{L,s}(x) < \min_{x \in \mathbb{B}_\infty(x_0,\epsilon)} \hat{f}_{L,s}(x). \tag{20}$$

If the two approaches share the same bounds of nodes of (k-1)-th layer, then:

$$\begin{aligned}\min_{x \in \mathbb{B}_\infty(x_0,\epsilon)} f_{L,s}(x) &= \min_{x \in \mathbb{B}_\infty(x_0,\epsilon)} \phi_{L,s}^k(x) \\ &= \sum_r w_{s,r}^k h_{L,r}^{k-1}(l_r^{k-1}) \\ &\ge \sum_r w_{s,r}^k \hat{h}_{L,r}^{k-1}(l_r^{k-1})\end{aligned}$$

which contradicts with (20). So the two approaches cannot share the same bounds, and there must be $\hat{l}_r^{k-1} > l_r^{k-1}$. Otherwise, $\hat{h}_{L,r}^{k-1}(\hat{l}_r^{k-1}) \le \sigma(\hat{l}_r^{k-1}) < \sigma(l_r^{k-1}) \le h_{L,r}^{k-1}(l_r^{k-1})$, meaning that (20) cannot be achieved. We have:

$$\begin{aligned}l_r^{k-1} &= \min_{x \in \mathbb{B}_\infty(x_0,\epsilon)} \phi_{L,r}^{k-1}(x) \\ &= \sum_j w_{r,j}^{k-1} h_{L,j}^{k-2}(l_j^{k-2}) \\ &< \hat{l}_r^{k-1} \\ &= \min_{x \in \mathbb{B}_\infty(x_0,\epsilon)} \hat{\phi}_{L,r}^{k-1}(x) \\ &= \sum_j w_{r,j}^{k-1} \hat{h}_{L,j}^{k-2}(\hat{l}_j^{k-2})\end{aligned}$$

Similarly, there must be $\hat{l}_j^{k-2} > l_j^{k-2}$ and so on. In the end, we can deduce that $\forall i \in [1, n], \hat{l}_i^0 > l_i^0$, which are the lower bounds of x_i. However, the input range of x_i is the same for the two approaches, which is a contradiction.

To conclude, there does not exist a $(\hat{f}_L, \hat{f}_U)$ satisfying (20). Theorem 2 is proven.

C ADDITIONAL EXPERIMENTAL RESULTS

This section presents the precision and efficiency comparison of NeWise with DeepCert, VeriNet and RobustVerifier on 27 Sigmoid, 30 Tanh, and 32 Arctan models with non-negative weights. In addition, we also demonstrated the effectiveness of Algorithm 1 on 40 1-hidden-layer models with mixed weights.

Table 6: Performance comparison on non-negative Sigmoid networks between NeWise (NW) and existing tools, DeepCert (DC), VeriNet (VN), and RobustVerifier (RV). $t \times n$ refers to an FNN with t layers and n neurons per layer. CNN_{t-c} denotes a CNN with t layers and c filters of size 3×3.

Dataset	Model	#Neur.	Certified Lower Bound														Time (s)
			Average							Standard Deviation							
			NW	DC	Impr. (%)	VN	Impr. (%)	RV	Impr. (%)	NW	DC	Impr. (%)	VN	Impr. (%)	RV	Impr. (%)	
MNIST	5x100	510	0.0091	0.0071	28.15 ↑	0.0071	27.25 ↑	0.0064	40.90 ↑	0.0057	0.0042	37.11 ↑	0.0042	35.48 ↑	0.0034	69.35 ↑	4.39 ±0.03
	3x700	2,110	0.0037	0.0030	24.92 ↑	0.0030	22.85 ↑	0.0029	27.05 ↑	0.0018	0.0013	41.86 ↑	0.0014	34.56 ↑	0.0013	41.86 ↑	117.50 ±0.22
	CNN_{6-5}	12,300	0.0968	0.0788	22.82 ↑	0.0778	24.37 ↑	0.0699	38.50 ↑	0.0372	0.0280	32.92 ↑	0.0276	35.09 ↑	0.0212	75.86 ↑	5.70 ±0.42
	3x50	160	0.0105	0.0088	19.23 ↑	0.0088	19.50 ↑	0.0080	31.42 ↑	0.0051	0.0038	32.72 ↑	0.0038	32.72 ↑	0.0029	71.86 ↑	0.14 ±0.00
	3x100	310	0.0139	0.0120	15.46 ↑	0.0120	15.56 ↑	0.0111	25.47 ↑	0.0071	0.0057	24.82 ↑	0.0057	23.30 ↑	0.0046	53.46 ↑	2.21 ±0.02
	CNN_{5-5}	10,680	0.0801	0.0708	13.14 ↑	0.0704	13.75 ↑	0.0683	17.30 ↑	0.0238	0.0200	18.87 ↑	0.0198	20.50 ↑	0.0180	32.20 ↑	2.89 ±0.31
	3x200	610	0.0080	0.0071	12.54 ↑	0.0071	12.85 ↑	0.0068	17.16 ↑	0.0046	0.0037	26.43 ↑	0.0037	25.41 ↑	0.0034	37.28 ↑	10.81 ±0.07
	3x400	1,210	0.0061	0.0056	9.66 ↑	0.0056	9.86 ↑	0.0054	12.89 ↑	0.0035	0.0030	16.78 ↑	0.0030	16.39 ↑	0.0028	26.09 ↑	39.52 ±0.09
	CNN_{3-2}	2,514	0.0521	0.0483	7.82 ↑	0.0483	7.94 ↑	0.0478	8.88 ↑	0.0180	0.0161	12.13 ↑	0.0160	12.41 ↑	0.0156	15.44 ↑	0.17 ±0.04
	CNN_{4-5}	8,680	0.0505	0.0473	6.68 ↑	0.0471	7.26 ↑	0.0464	8.81 ↑	0.0207	0.0186	11.26 ↑	0.0183	12.84 ↑	0.0175	17.87 ↑	1.17 ±0.20
	CNN_{3-4}	5,018	0.0448	0.0422	6.09 ↑	0.0421	6.24 ↑	0.0418	6.98 ↑	0.0156	0.0142	9.71 ↑	0.0141	10.18 ↑	0.0138	12.56 ↑	0.30 ±0.08
Fashion MNIST	4x100	410	0.0312	0.0188	65.48 ↑	0.0194	60.62 ↑	0.0159	96.22 ↑	0.0403	0.0210	92.28 ↑	0.0220	83.20 ↑	0.0176	129.47 ↑	3.34 ±0.02
	3x100	310	0.0326	0.0263	24.02 ↑	0.0270	21.03 ↑	0.0238	36.81 ↑	0.0335	0.0262	27.67 ↑	0.0282	18.92 ↑	0.0234	43.22 ↑	2.24 ±0.02
	2x100	210	0.0306	0.0250	22.49 ↑	0.0254	20.51 ↑	0.0230	33.09 ↑	0.0286	0.0211	36.04 ↑	0.0228	25.88 ↑	0.0194	47.76 ↑	1.13 ±0.01
	3x200	610	0.0223	0.0184	21.80 ↑	0.0187	19.45 ↑	0.0170	31.70 ↑	0.0220	0.0159	38.66 ↑	0.0170	29.38 ↑	0.0143	54.42 ↑	9.20 ±2.00
	2x200	410	0.0263	0.0220	19.52 ↑	0.0223	17.86 ↑	0.0204	28.77 ↑	0.0279	0.0200	39.55 ↑	0.0211	31.96 ↑	0.0176	58.76 ↑	3.60 ±0.02
	CNN_{5-5}	10,680	0.1303	0.1155	12.81 ↑	0.1151	13.22 ↑	0.1088	19.72 ↑	0.0830	0.0714	16.23 ↑	0.0721	15.10 ↑	0.0636	30.51 ↑	2.90 ±0.33
	CNN_{3-2}	2,514	0.0790	0.0713	10.79 ↑	0.0713	10.74 ↑	0.0695	13.68 ↑	0.0497	0.0416	19.55 ↑	0.0418	19.06 ↑	0.0386	28.98 ↑	0.17 ±0.04
	CNN_{4-5}	8,680	0.0959	0.0868	10.40 ↑	0.0864	10.90 ↑	0.0839	14.19 ↑	0.0561	0.0486	15.51 ↑	0.0482	16.52 ↑	0.0453	24.03 ↑	1.18 ±0.21
	CNN_{3-4}	5,018	0.0747	0.0694	7.52 ↑	0.0693	7.72 ↑	0.0681	9.70 ↑	0.0465	0.0410	13.32 ↑	0.0409	13.59 ↑	0.0391	18.85 ↑	0.30 ±0.09
CIFAR10	9x100	910	0.0315	0.0211	49.03 ↑	0.0214	46.94 ↑	0.0192	63.58 ↑	0.0280	0.0183	52.70 ↑	0.0186	50.32 ↑	0.0133	110.07 ↑	4.93 ±0.02
	6x100	610	0.0221	0.0174	27.08 ↑	0.0176	26.14 ↑	0.0170	30.22 ↑	0.0165	0.0118	40.05 ↑	0.0120	37.82 ↑	0.0111	48.24 ↑	3.04 ±0.02
	5x100	510	0.0200	0.0167	19.76 ↑	0.0167	19.47 ↑	0.0163	22.40 ↑	0.0137	0.0104	31.80 ↑	0.0104	31.42 ↑	0.0099	38.45 ↑	2.44 ±0.01
	3x50	160	0.0206	0.0178	15.43 ↑	0.0179	14.66 ↑	0.0176	16.88 ↑	0.0144	0.0113	27.57 ↑	0.0115	25.24 ↑	0.0110	31.30 ↑	0.43 ±0.00
	4x100	410	0.0161	0.0140	15.23 ↑	0.0140	14.81 ↑	0.0138	16.56 ↑	0.0111	0.0089	24.61 ↑	0.0090	23.63 ↑	0.0087	27.62 ↑	1.87 ±0.03
	CNN_{3-4}	6,746	0.0187	0.0181	3.38 ↑	0.0181	3.32 ↑	0.0181	3.43 ↑	0.0109	0.0103	5.93 ↑	0.0103	5.83 ↑	0.0103	6.13 ↑	0.56 ±0.08
	CNN_{3-2}	3,378	0.0185	0.0180	2.49 ↑	0.0180	2.55 ↑	0.0180	2.67 ↑	0.0125	0.0120	4.34 ↑	0.0120	4.34 ↑	0.0120	4.60 ↑	0.30 ±0.05

Table 7: Performance comparison of NeWise (NW) with DeepCert (DC), VeriNet (VN), and RobustVerifier (RV) on non-negative Tanh networks. $t \times n$ refers to an FNN with t layers and n neurons per layer. CNN_{t-c} denotes a CNN with t layers and c filters of size 3×3.

Dataset	Model	#Neur.	Certified Lower Bound														Time (s)
			Average							Standard Deviation							
			NW	DC	Impr. (%)	VN	Impr. (%)	RV	Impr. (%)	NW	DC	Impr. (%)	VN	Impr. (%)	RV	Impr. (%)	
MNIST	5x100	510	0.0032	0.0012	173.28 ↑	0.0013	145.74 ↑	0.0010	207.77 ↑	0.0018	0.0005	233.96 ↑	0.0006	195.00 ↑	0.0006	216.07 ↑	4.36 ± 0.06
	3x700	2,110	0.0044	0.0016	170.99 ↑	0.0018	141.21 ↑	0.0016	174.38 ↑	0.0027	0.0008	251.28 ↑	0.0009	191.49 ↑	0.0009	191.49 ↑	117.43 ± 0.14
	3x400	1,210	0.0038	0.0017	119.65 ↑	0.0019	95.88 ↑	0.0016	130.30 ↑	0.0018	0.0007	166.67 ↑	0.0008	128.57 ↑	0.0007	137.84 ↑	39.45 ± 0.14
	CNN_{6-5}	12,300	0.0601	0.0358	67.98 ↑	0.0381	57.67 ↑	0.0303	98.61 ↑	0.0243	0.0115	111.84 ↑	0.0131	85.94 ↑	0.0087	179.13 ↑	5.74 ± 0.46
	3x50	160	0.0027	0.0023	18.78 ↑	0.0023	17.24 ↑	0.0022	25.35 ↑	0.0012	0.0009	29.79 ↑	0.0010	27.08 ↑	0.0008	45.24 ↑	0.14 ± 0.00
	3x100	310	0.0033	0.0029	15.97 ↑	0.0029	14.78 ↑	0.0027	21.45 ↑	0.0014	0.0011	23.85 ↑	0.0011	19.47 ↑	0.0010	33.66 ↑	2.17 ± 0.03
	3x200	610	0.0031	0.0027	15.41 ↑	0.0027	14.13 ↑	0.0026	18.99 ↑	0.0013	0.0011	26.42 ↑	0.0011	19.64 ↑	0.0010	31.37 ↑	7.54 ± 1.00
	CNN_{3-4}	5,018	0.0234	0.0208	12.48 ↑	0.0213	9.94 ↑	0.0209	12.21 ↑	0.0067	0.0055	21.05 ↑	0.0058	14.80 ↑	0.0055	20.83 ↑	0.33 ± 0.09
	CNN_{5-5}	10,680	0.0329	0.0294	11.92 ↑	0.0296	10.93 ↑	0.0290	13.42 ↑	0.0108	0.0090	20.24 ↑	0.0092	17.50 ↑	0.0087	24.54 ↑	2.91 ± 0.31
	CNN_{4-5}	8,680	0.0272	0.0241	13.08 ↑	0.0244	11.51 ↑	0.0239	14.03 ↑	0.0074	0.0061	21.21 ↑	0.0063	17.19 ↑	0.0060	23.63 ↑	1.19 ± 0.19
	CNN_{3-2}	2,514	0.0327	0.0289	13.08 ↑	0.0294	11.35 ↑	0.0288	13.63 ↑	0.0100	0.0082	21.90 ↑	0.0085	17.33 ↑	0.0081	23.10 ↑	0.18 ± 0.04
Fashion MNIST	3x100	310	0.0153	0.0114	34.39 ↑	0.0117	30.72 ↑	0.0103	48.02 ↑	0.0156	0.0105	48.81 ↑	0.0110	42.04 ↑	0.0091	70.79 ↑	2.20 ± 0.01
	2x200	410	0.0099	0.0082	21.42 ↑	0.0083	19.23 ↑	0.0079	25.57 ↑	0.0102	0.0076	33.38 ↑	0.0080	27.06 ↑	0.0076	33.55 ↑	5.42 ± 0.03
	CNN_{6-5}	12,300	0.0408	0.0334	22.36 ↑	0.0343	19.18 ↑	0.0296	37.67 ↑	0.0329	0.0237	38.83 ↑	0.0242	35.67 ↑	0.0180	82.66 ↑	5.79 ± 0.50
	2x100	210	0.0108	0.0090	19.69 ↑	0.0092	17.60 ↑	0.0086	25.85 ↑	0.0109	0.0081	35.27 ↑	0.0085	28.59 ↑	0.0077	41.95 ↑	1.12 ± 0.01
	CNN_{5-5}	10,680	0.0305	0.0256	18.88 ↑	0.0264	15.55 ↑	0.0239	27.28 ↑	0.0201	0.0153	31.52 ↑	0.0158	27.03 ↑	0.0125	60.69 ↑	2.92 ± 0.34
	CNN_{4-5}	8,680	0.0276	0.0230	20.08 ↑	0.0240	15.22 ↑	0.0223	24.07 ↑	0.0188	0.0134	41.12 ↑	0.0139	35.83 ↑	0.0129	45.82 ↑	1.22 ± 0.22
	CNN_{3-2}	2,514	0.0271	0.0233	15.85 ↑	0.0242	11.68 ↑	0.0234	15.45 ↑	0.0111	0.0087	28.49 ↑	0.0091	22.42 ↑	0.0085	31.37 ↑	0.18 ± 0.04
	CNN_{3-4}	5,018	0.0302	0.0264	14.19 ↑	0.0271	11.32 ↑	0.0263	14.88 ↑	0.0160	0.0126	27.29 ↑	0.0130	23.36 ↑	0.0121	32.45 ↑	0.31 ± 0.09
	3x200	610	0.0529	0.0430	23.17 ↑	0.0440	20.23 ↑	0.0354	49.70 ↑	0.0662	0.0550	20.29 ↑	0.0563	17.43 ↑	0.0454	45.67 ↑	10.77 ± 0.05
CIFAR10	3x200	610	0.0226	0.0127	78.69 ↑	0.0137	65.86 ↑	0.0120	88.82 ↑	0.0176	0.0083	113.30 ↑	0.0092	90.91 ↑	0.0080	119.40 ↑	6.04 ± 0.85
	4x100	410	0.0198	0.0094	111.29 ↑	0.0106	88.06 ↑	0.0091	118.98 ↑	0.0146	0.0081	79.75 ↑	0.0101	45.63 ↑	0.0097	51.19 ↑	1.84 ± 0.00
	3x700	2,110	0.0688	0.0364	89.11 ↑	0.0391	76.09 ↑	0.0384	78.93 ↑	0.0512	0.0377	35.99 ↑	0.0386	32.64 ↑	0.0406	26.33 ↑	103.08 ± 0.06
	3x400	1,210	0.0484	0.0256	89.00 ↑	0.0295	64.15 ↑	0.0256	88.85 ↑	0.0441	0.0245	79.67 ↑	0.0291	51.58 ↑	0.0253	74.69 ↑	35.79 ± 0.05
	3x100	310	0.0429	0.0273	57.37 ↑	0.0295	45.33 ↑	0.0269	59.42 ↑	0.0435	0.0243	78.79 ↑	0.0270	61.35 ↑	0.0256	69.66 ↑	1.26 ± 0.00
	5x100	510	0.0462	0.0299	54.64 ↑	0.0315	46.45 ↑	0.0300	54.12 ↑	0.0400	0.0372	7.58 ↑	0.0378	5.96 ↑	0.0378	5.87 ↑	2.43 ± 0.01
	3x50	160	0.0170	0.0135	25.94 ↑	0.0138	23.30 ↑	0.0134	27.26 ↑	0.0111	0.0073	53.52 ↑	0.0077	44.73 ↑	0.0071	56.32 ↑	0.43 ± 0.00
	CNN_{3-2}	3,378	0.0136	0.0134	1.49 ↑	0.0134	1.49 ↑	0.0134	1.56 ↑	0.0106	0.0102	4.01 ↑	0.0102	4.01 ↑	0.0102	4.21 ↑	0.31 ± 0.06
	CNN_{3-4}	6,746	0.0102	0.0101	0.89 ↑	0.0101	0.99 ↑	0.0101	0.99 ↑	0.0062	0.0061	1.80 ↑	0.0061	1.80 ↑	0.0061	1.96 ↑	0.59 ± 0.12
	CNN_{3-5}	8,430	0.0094	0.0093	0.97 ↑	0.0093	0.97 ↑	0.0093	0.97 ↑	0.0066	0.0065	1.86 ↑	0.0065	1.86 ↑	0.0065	2.02 ↑	0.75 ± 0.15

Table 8: Comparison on non-negative Arctan networks.

Dataset	Model	#Neur.	Certified Lower Bound														Time (s)
			Average							Standard Deviation							
			NW	DC	Impr. (%)	VN	Impr. (%)	RV	Impr. (%)	NW	DC	Impr. (%)	VN	Impr. (%)	RV	Impr. (%)	
MNIST	CNN_{6-5}	12,300	0.0484	0.0262	84.78 ↑	0.0367	32.11 ↑	0.0325	49.15 ↑	0.0189	0.0072	162.78 ↑	0.0124	52.21 ↑	0.0098	92.67 ↑	5.57 ±0.05
	5x100	510	0.0020	0.0012	73.28 ↑	0.0015	29.68 ↑	0.0014	41.55 ↑	0.0012	0.0005	144.00 ↑	0.0008	48.78 ↑	0.0007	67.12 ↑	4.36 ±0.02
	3x700	2,110	0.0022	0.0015	47.06 ↑	0.0019	20.32 ↑	0.0017	29.31 ↑	0.0012	0.0007	58.11 ↑	0.0009	28.57 ↑	0.0008	42.68 ↑	117.69 ±0.24
	3x50	160	0.0051	0.0037	36.83 ↑	0.0043	18.10 ↑	0.0040	26.62 ↑	0.0026	0.0017	51.15 ↑	0.0020	32.83 ↑	0.0017	52.91 ↑	0.14 ±0.00
	3x400	1,210	0.0024	0.0017	39.64 ↑	0.0020	17.41 ↑	0.0019	24.21 ↑	0.0011	0.0007	61.76 ↑	0.0009	26.44 ↑	0.0008	37.50 ↑	39.59 ±0.13
	3x200	610	0.0028	0.0021	36.23 ↑	0.0024	16.53 ↑	0.0023	22.08 ↑	0.0012	0.0008	50.00 ↑	0.0010	28.12 ↑	0.0009	41.38 ↑	10.68 ±0.04
	3x100	310	0.0031	0.0023	32.76 ↑	0.0027	14.93 ↑	0.0026	19.84 ↑	0.0013	0.0009	42.05 ↑	0.0010	22.55 ↑	0.0009	31.58 ↑	2.21 ±0.03
	CNN_{5-5}	10,680	0.0218	0.0162	34.24 ↑	0.0196	11.22 ↑	0.0191	14.02 ↑	0.0069	0.0043	62.38 ↑	0.0059	18.80 ↑	0.0055	26.59 ↑	2.79 ±0.05
	CNN_{3-2}	2,514	0.0138	0.0103	34.66 ↑	0.0127	8.90 ↑	0.0124	11.08 ↑	0.0042	0.0027	56.88 ↑	0.0037	12.83 ↑	0.0036	17.88 ↑	0.16 ±0.01
	CNN_{4-5}	8,680	0.0203	0.0158	28.08 ↑	0.0186	9.05 ↑	0.0182	11.20 ↑	0.0068	0.0045	52.00 ↑	0.0059	15.15 ↑	0.0057	20.85 ↑	1.12 ±0.03
	CNN_{3-4}	5,018	0.0162	0.0130	24.71 ↑	0.0152	6.51 ↑	0.0151	7.57 ↑	0.0053	0.0037	42.28 ↑	0.0048	9.83 ↑	0.0047	12.66 ↑	0.28 ±0.02
Fashion MNIST	4x100	410	0.0179	0.0084	112.98 ↑	0.0108	66.26 ↑	0.0092	94.88 ↑	0.0279	0.0118	136.19 ↑	0.0150	85.31 ↑	0.0134	107.68 ↑	3.20 ±0.02
	3x100	310	0.0120	0.0078	53.98 ↑	0.0091	31.07 ↑	0.0081	47.17 ↑	0.0127	0.0076	66.80 ↑	0.0089	42.41 ↑	0.0078	63.14 ↑	2.13 ±0.01
	3x200	610	0.0097	0.0067	44.68 ↑	0.0077	25.49 ↑	0.0071	36.49 ↑	0.0107	0.0073	45.37 ↑	0.0081	31.89 ↑	0.0070	52.43 ↑	8.90 ±1.88
	2x100	210	0.0105	0.0082	27.95 ↑	0.0091	16.35 ↑	0.0086	23.01 ↑	0.0095	0.0069	37.19 ↑	0.0074	28.11 ↑	0.0069	37.99 ↑	1.08 ±0.01
	CNN_{6-5}	12,300	0.0324	0.0228	42.16 ↑	0.0282	14.95 ↑	0.0258	25.88 ↑	0.0228	0.0157	45.14 ↑	0.0180	27.19 ↑	0.0134	69.87 ↑	5.63 ±0.16
	2x200	410	0.0086	0.0069	24.82 ↑	0.0076	13.97 ↑	0.0073	18.82 ↑	0.0079	0.0062	28.04 ↑	0.0065	20.98 ↑	0.0061	29.08 ↑	4.50 ±0.92
	CNN_{3-2}	2,514	0.0266	0.0190	40.32 ↑	0.0235	13.34 ↑	0.0225	17.97 ↑	0.0179	0.0105	71.41 ↑	0.0127	41.29 ↑	0.0115	55.37 ↑	0.16 ±0.01
	CNN_{4-5}	8,680	0.0241	0.0176	37.07 ↑	0.0217	10.82 ↑	0.0207	16.06 ↑	0.0117	0.0086	36.96 ↑	0.0099	17.93 ↑	0.0090	30.40 ↑	1.14 ±0.06
	CNN_{5-5}	10,680	0.0266	0.0201	32.22 ↑	0.0241	10.50 ↑	0.0228	16.95 ↑	0.0121	0.0097	24.77 ↑	0.0107	13.88 ↑	0.0099	22.75 ↑	2.81 ±0.08
	CNN_{3-4}	5,018	0.0258	0.0205	26.05 ↑	0.0237	8.64 ↑	0.0231	11.60 ↑	0.0158	0.0114	38.50 ↑	0.0135	17.61 ↑	0.0124	27.97 ↑	0.29 ±0.02
CIFAR10	4x100	410	0.0173	0.0145	19.30 ↑	0.0158	9.70 ↑	0.0156	11.25 ↑	0.0128	0.0100	27.86 ↑	0.0110	16.11 ↑	0.0107	19.59 ↑	1.83 ±0.01
	5x100	510	0.0248	0.0213	16.67 ↑	0.0229	8.28 ↑	0.0227	9.38 ↑	0.0195	0.0167	17.16 ↑	0.0176	11.16 ↑	0.0173	13.09 ↑	2.42 ±0.00
	3x50	160	0.0186	0.0158	17.17 ↑	0.0171	8.41 ↑	0.0169	9.82 ↑	0.0112	0.0092	22.04 ↑	0.0099	13.42 ↑	0.0096	17.45 ↑	0.43 ±0.00
	6x100	610	0.0171	0.0148	15.64 ↑	0.0159	7.69 ↑	0.0158	8.44 ↑	0.0157	0.0139	12.72 ↑	0.0144	9.19 ↑	0.0142	10.42 ↑	3.03 ±0.01
	3x100	310	0.0138	0.0119	15.71 ↑	0.0127	8.17 ↑	0.0126	9.29 ↑	0.0113	0.0094	20.53 ↑	0.0100	13.30 ↑	0.0098	15.85 ↑	1.26 ±0.01
	3x200	610	0.0107	0.0095	12.92 ↑	0.0101	6.23 ↑	0.0101	6.86 ↑	0.0073	0.0061	19.12 ↑	0.0066	10.12 ↑	0.0065	11.47 ↑	6.33 ±0.01
	3x700	2,110	0.0079	0.0070	13.12 ↑	0.0075	5.73 ↑	0.0074	6.59 ↑	0.0053	0.0044	19.33 ↑	0.0049	9.03 ↑	0.0048	10.63 ↑	102.47 ±0.14
	3x400	1,210	0.0105	0.0094	12.06 ↑	0.0099	5.74 ↑	0.0099	6.38 ↑	0.0068	0.0058	17.76 ↑	0.0062	9.46 ↑	0.0062	10.88 ↑	37.85 ±0.02
	CNN_{3-2}	3,378	0.0115	0.0113	1.77 ↑	0.0114	0.88 ↑	0.0114	0.88 ↑	0.0078	0.0076	3.02 ↑	0.0077	1.55 ↑	0.0077	1.69 ↑	0.29 ±0.02
	CNN_{3-4}	6,746	0.0080	0.0079	1.53 ↑	0.0079	0.88 ↑	0.0079	0.88 ↑	0.0051	0.0049	2.84 ↑	0.0050	1.40 ↑	0.0050	1.60 ↑	0.55 ±0.03
	CNN_{3-5}	8,430	0.0095	0.0094	1.39 ↑	0.0094	0.64 ↑	0.0094	0.64 ↑	0.0060	0.0059	2.72 ↑	0.0060	1.17 ↑	0.0060	1.34 ↑	0.70 ±0.03

Table 9: Performance comparison of Alg. 1 with DeepCert (DC), VeriNet (VN), and RobustVerifier (RV) on 1-hidden-layer Sigmoid and Tanh networks with mixed weights.

Arch.	Model	σ	Certified Lower Bound														Time (s)	
			Average							Standard Deviation							Alg.1	Others
			Alg.1	DC	Impr. (%)	VN	Impr. (%)	RV	Impr. (%)	Alg.1	DC	Impr. (%)	VN	Impr. (%)	RV	Impr. (%)		
CNN	CNN_{2-1-5}^{*}	Sig.	0.0706	0.0437	61.39 ↑	0.0435	62.32 ↑	0.0428	64.90 ↑	0.0306	0.0145	110.32 ↑	0.0143	114.30 ↑	0.0137	122.57 ↑	0.56	0.06 ±0.01
		Tanh	0.0489	0.0286	71.06 ↑	0.0285	71.54 ↑	0.0277	76.74 ↑	0.0227	0.0132	71.32 ↑	0.0132	72.10 ↑	0.0121	87.00 ↑	0.59	0.06 ±0.01
	CNN_{2-2-5}^{*}	Sig.	0.0749	0.0541	38.29 ↑	0.0539	38.98 ↑	0.0521	43.79 ↑	0.0312	0.0208	49.97 ↑	0.0207	51.14 ↑	0.0187	66.63 ↑	1.19	0.08 ±0.01
		Tanh	0.0449	0.0332	35.03 ↑	0.0331	35.48 ↑	0.0321	39.91 ↑	0.0204	0.0123	66.19 ↑	0.0122	67.15 ↑	0.0113	80.64 ↑	1.22	0.08 ±0.01
	CNN_{2-3-5}^{*}	Sig.	0.0689	0.0526	31.03 ↑	0.0524	31.48 ↑	0.0503	37.03 ↑	0.0279	0.0197	41.45 ↑	0.0196	41.88 ↑	0.0176	58.60 ↑	1.75	0.09 ±0.02
		Tanh	0.0444	0.0327	35.84 ↑	0.0326	36.05 ↑	0.0317	40.26 ↑	0.0182	0.0121	50.90 ↑	0.0120	51.15 ↑	0.0111	63.94 ↑	1.99	0.10 ±0.02
	CNN_{2-4-5}^{*}	Sig.	0.0915	0.0647	41.39 ↑	0.0645	41.81 ↑	0.0621	47.43 ↑	0.0405	0.0233	73.73 ↑	0.0232	74.55 ↑	0.0210	92.76 ↑	2.54	0.11 ±0.02
		Tanh	0.0446	0.0272	63.87 ↑	0.0272	64.06 ↑	0.0266	67.95 ↑	0.0184	0.0103	78.91 ↑	0.0103	78.91 ↑	0.0096	91.81 ↑	2.38	0.11 ±0.03
	CNN_{2-5-3}^{*}	Sig.	0.0682	0.0477	42.81 ↑	0.0476	43.11 ↑	0.0471	44.81 ↑	0.0349	0.0182	91.53 ↑	0.0182	92.27 ↑	0.0176	98.50 ↑	2.57	0.09 ±0.03
		Tanh	0.0289	0.0192	50.28 ↑	0.0192	50.52 ↑	0.0191	51.62 ↑	0.0134	0.0073	85.10 ↑	0.0072	85.86 ↑	0.0071	89.81 ↑	2.93	0.10 ±0.03
	CNN_{2-1-5}^{+}	Sig.	0.1013	0.0877	15.47 ↑	0.0876	15.56 ↑	0.0835	21.28 ↑	0.0506	0.0385	31.58 ↑	0.0386	31.24 ↑	0.0348	45.29 ↑	0.43	0.06 ±0.01
		Tanh	0.0658	0.0555	18.58 ↑	0.0554	18.82 ↑	0.0525	25.36 ↑	0.0349	0.0253	37.89 ↑	0.0254	37.62 ↑	0.0227	54.06 ↑	0.57	0.06 ±0.01
	CNN_{2-2-5}^{+}	Sig.	0.1045	0.0823	26.99 ↑	0.0822	27.05 ↑	0.0777	34.47 ↑	0.0574	0.0353	62.46 ↑	0.0355	61.59 ↑	0.0311	84.39 ↑	0.80	0.08 ±0.01
		Tanh	0.0629	0.0536	17.39 ↑	0.0535	17.52 ↑	0.0509	23.62 ↑	0.0354	0.0260	36.39 ↑	0.0260	36.13 ↑	0.0233	51.69 ↑	0.71	0.08 ±0.02
	CNN_{2-3-5}^{+}	Sig.	0.1036	0.0843	22.77 ↑	0.0843	22.79 ↑	0.0811	27.72 ↑	0.0509	0.0371	37.06 ↑	0.0374	36.07 ↑	0.0344	47.89 ↑	1.56	0.09 ±0.02
		Tanh	0.0699	0.0507	38.00 ↑	0.0506	38.22 ↑	0.0478	46.07 ↑	0.0404	0.0245	65.28 ↑	0.0245	65.35 ↑	0.0215	88.02 ↑	1.38	0.10 ±0.02
	CNN_{2-4-5}^{+}	Sig.	0.1040	0.0814	27.76 ↑	0.0814	27.81 ↑	0.0784	32.73 ↑	0.0587	0.0366	60.43 ↑	0.0367	59.91 ↑	0.0336	74.50 ↑	1.80	0.11 ±0.02
		Tanh	0.0713	0.0519	37.43 ↑	0.0518	37.59 ↑	0.0494	44.19 ↑	0.0447	0.0246	81.51 ↑	0.0246	81.81 ↑	0.0219	104.05 ↑	1.84	0.11 ±0.03
	CNN_{2-5-3}^{+}	Sig.	0.0922	0.0700	31.65 ↑	0.0699	31.84 ↑	0.0678	36.00 ↑	0.0485	0.0340	42.87 ↑	0.0340	42.66 ↑	0.0312	55.36 ↑	2.33	0.09 ±0.04
		Tanh	0.0520	0.0336	54.99 ↑	0.0335	55.18 ↑	0.0325	60.25 ↑	0.0389	0.0183	112.18 ↑	0.0184	112.06 ↑	0.0167	133.72 ↑	2.78	0.10 ±0.04
FNN	1x50*	Sig.	0.0357	0.0275	29.65 ↑	0.0279	27.98 ↑	0.0235	51.64 ↑	0.0121	0.0082	47.17 ↑	0.0085	41.97 ↑	0.0062	93.70 ↑	0.33	0.03 ±0.00
		Tanh	0.0241	0.0197	22.49 ↑	0.0199	21.25 ↑	0.0167	44.60 ↑	0.0077	0.0056	36.69 ↑	0.0058	32.44 ↑	0.0042	82.26 ↑	0.29	0.03 ±0.00
	1x100*	Sig.	0.0324	0.0247	31.15 ↑	0.0250	29.73 ↑	0.0215	50.72 ↑	0.0104	0.0064	63.11 ↑	0.0066	56.72 ↑	0.0050	108.97 ↑	0.40	0.04 ±0.00
		Tanh	0.0219	0.0177	23.47 ↑	0.0179	22.23 ↑	0.0152	43.94 ↑	0.0077	0.0049	57.37 ↑	0.0050	52.69 ↑	0.0037	107.43 ↑	0.33	0.05 ±0.01
	1x150*	Sig.	0.0373	0.0290	28.59 ↑	0.0292	27.71 ↑	0.0254	46.55 ↑	0.0133	0.0083	60.57 ↑	0.0085	55.68 ↑	0.0064	107.16 ↑	0.36	0.06 ±0.00
		Tanh	0.0238	0.0197	20.81 ↑	0.0198	20.02 ↑	0.0171	39.50 ↑	0.0076	0.0055	39.20 ↑	0.0056	35.96 ↑	0.0042	80.43 ↑	0.37	0.06 ±0.00
	1x200*	Sig.	0.0343	0.0260	31.83 ↑	0.0261	31.17 ↑	0.0230	48.94 ↑	0.0117	0.0074	57.83 ↑	0.0076	54.49 ↑	0.0058	102.41 ↑	0.38	0.07 ±0.00
		Tanh	0.0228	0.0183	24.64 ↑	0.0184	24.03 ↑	0.0162	41.08 ↑	0.0077	0.0044	74.74 ↑	0.0045	70.51 ↑	0.0035	121.17 ↑	0.38	0.07 ±0.01
	1x250*	Sig.	0.0364	0.0256	42.34 ↑	0.0257	41.84 ↑	0.0229	58.86 ↑	0.0117	0.0075	56.87 ↑	0.0076	54.38 ↑	0.0060	95.76 ↑	0.44	0.09 ±0.00
		Tanh	0.0240	0.0166	45.03 ↑	0.0166	44.51 ↑	0.0147	63.37 ↑	0.0083	0.0040	107.56 ↑	0.0040	103.98 ↑	0.0031	163.09 ↑	0.44	0.09 ±0.00
	1x50+	Sig.	0.0451	0.0351	28.50 ↑	0.0356	26.73 ↑	0.0292	54.40 ↑	0.0193	0.0117	64.36 ↑	0.0122	58.29 ↑	0.0089	117.29 ↑	0.27	0.03 ±0.00
		Tanh	0.0300	0.0235	27.89 ↑	0.0237	26.54 ↑	0.0193	55.70 ↑	0.0109	0.0078	39.12 ↑	0.0081	33.97 ↑	0.0057	91.05 ↑	0.27	0.03 ±0.00
	1x100+	Sig.	0.0421	0.0331	27.37 ↑	0.0334	26.07 ↑	0.0276	52.89 ↑	0.0169	0.0119	41.35 ↑	0.0123	37.77 ↑	0.0088	92.66 ↑	0.31	0.04 ±0.00
		Tanh	0.0260	0.0212	22.61 ↑	0.0213	21.75 ↑	0.0177	46.97 ↑	0.0109	0.0066	64.37 ↑	0.0068	60.72 ↑	0.0048	125.28 ↑	0.36	0.05 ±0.01
	1x150+	Sig.	0.0460	0.0375	22.63 ↑	0.0377	21.81 ↑	0.0317	44.99 ↑	0.0188	0.0120	56.68 ↑	0.0123	53.11 ↑	0.0090	108.74 ↑	0.35	0.06 ±0.00
		Tanh	0.0303	0.0238	27.49 ↑	0.0239	26.80 ↑	0.0198	53.29 ↑	0.0107	0.0077	38.42 ↑	0.0078	35.95 ↑	0.0056	90.58 ↑	0.41	0.06 ±0.00
	1x200+	Sig.	0.0484	0.0378	28.11 ↑	0.0380	27.24 ↑	0.0318	52.02 ↑	0.0181	0.0129	40.47 ↑	0.0132	37.38 ↑	0.0096	89.04 ↑	0.37	0.07 ±0.00
		Tanh	0.0295	0.0228	29.45 ↑	0.0229	28.77 ↑	0.0192	53.64 ↑	0.0107	0.0074	44.50 ↑	0.0075	42.20 ↑	0.0056	93.18 ↑	0.40	0.07 ±0.00
	1x250+	Sig.	0.0474	0.0385	23.06 ↑	0.0387	22.52 ↑	0.0326	45.16 ↑	0.0185	0.0126	46.20 ↑	0.0128	44.26 ↑	0.0095	93.20 ↑	0.41	0.09 ±0.00
		Tanh	0.0263	0.0225	16.84 ↑	0.0226	16.37 ↑	0.0191	37.67 ↑	0.0103	0.0066	55.62 ↑	0.0067	53.30 ↑	0.0049	111.66 ↑	0.44	0.09 ±0.00